Supporting Information

Exchange Speed of Four-component Nanorotors Correlates with Hammett Substituent Constants

Yi-Fan Li, Amit Ghosh, Pronay Kumar Biswas, Suchismita Saha, Michael Schmittel*

Center of Micro and Nanochemistry and Engineering, Organische Chemie I, Universität Siegen, Adolf-Reichwein-Str.2, D-57068 Siegen, Germany

E-mail: schmittel@chemie.uni-siegen.de

Table of contents

1. Synthesis

1.1. General Information

All solvents were dried by distillation prior to use while commercial reagents (**8**, **9**, **10**, **13**, **15**) were used without any further purification. Bruker Avance (400 MHz), JEOL (500 MHz) and Varian (600 MHz) spectrometers were used to measure ^{1}H and ^{13}C NMR spectra using a deuterated solvent as the lock and residual protiated solvent as internal reference ($CDCl_3$: δ_H 7.26 ppm, δ_C 77.0 ppm; CD_2Cl_2: δ_H 5.32 ppm, δ_C 53.8 ppm; THF-d_8: δ_H 1.72 ppm, 3.58 ppm, δ_C 25.3 ppm, 67.2 ppm). The following abbreviations were used to define NMR peak pattern: s = singlet, d = doublet, t = triplet, dd = doublet of doublets, ddd = doublet of doublets of doublets, dt = doublet of triplets, td = triplet of doublets, brs = broad signal, m = multiplet. The coupling constant values are given in Hertz (Hz). Wherever possible, assignments of protons, are provided. The numbering of the carbons in different molecular skeletons was not guided by IUPAC nomenclature rules; it was exclusively done for assigning NMR signals. All electrospray ionization (ESI-MS) spectra were recorded on a Thermo-Quest LCQ deca and the theoretical isotopic distributions of the mass signals were calculated using IsoPro 3.0 software. Melting points were measured on a BÜCHI 510 instrument and are not corrected. Infrared spectra were recorded on a Perkin Elmer Spectrum-Two FT-IR spectrometer. Elemental analysis was performed using the EA-3000 CHNS analyzer. UV-vis spectra were recorded on a Cary Win 50 (298 K) spectrometer. Binding constants were determined through UV-vis titrations in combination with a 1:1 binding formula of two ligands or with SPECFIT/32TM global analysis system by Spectrum Software Associates (Marlborough, MA). Column chromatography was performed either on silica gel (60-400 mesh) or neutral alumina (Fluka, 0.05-0.15 mm, Brockmann Activity 1). Merck silica gel (60 F_{254}) or neutral alumina (150 F_{254}) sheets were used for thin layer chromatography (TLC). Preparation of metal complexes was performed directly in the NMR tube using CD_2Cl_2 as solvent. Compounds **11**,[1] **12**,[2] **14**,[3] and **20**[4] were synthesized according to literature known procedures.

1.2. Synthesis and Characterization of Ligands

Zinc(II)-5-[4-(5-methoxy-3-pyridylethynyl)phenyl]-10,15,20-trimesitylporphyrin (1)

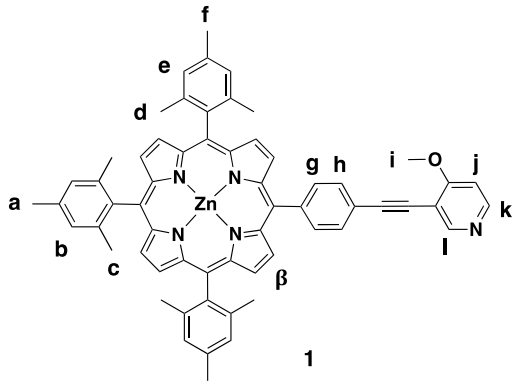

Zinc(II)-5-(4-ethynylphenyl)-10,15,20-trimesitylporphyrin (**11**, 200 mg, 242 μmol) and 3-bromo-4-methoxypyridine (**8**, 250 mg, 1.35 mmol) were dissolved in dry DMF (20.0 mL) and dry Et_3N (40.0 mL) and the solution was degassed by using two freeze-pump-thaw cycles. Then, $Pd(PPh_3)_4$ (31.0 mg, 30.0 μmol) was added under N_2 atmosphere. One additional freeze-pump-thaw cycle was applied for degassing. The mixture was stirred at 80 °C for 14 h (CAUTION: sealed tube). After evaporation of the solvent under reduced pressure and work up with ice water and CH_2Cl_2, the crude product was dried over anhydrous Na_2SO_4 and concentrated under reduced pressure. Thereafter, the crude product was separated by column chromatography on silica gel using THF. Further purification was achieved by size exclusion chromatography using SX-3 biobead and THF affording **1** as a purple solid (187 mg, 201 μmol, 83%). $\boldsymbol{R_f}$ = 0.5 (SiO_2, CH_2Cl_2). **MP:** > 300 °C **^{1}H NMR (THF-d_8, 500 MHz):** δ = 8.77 (d, ^3J = 4.6 Hz, 2H, β -H), 8.64 (d, ^3J = 4.6 Hz, 2H, β -H), 8.60 (s, 4H, β-H), 8.44 (s, 1H, l-H), 8.25 (d, ^3J = 5.8 Hz, 1H, k-H), 8.20 (d, ^3J = 8.1 Hz, 2H, h-H), 7.88 (d, ^3J = 8.1 Hz, 2H, g-H), 7.28 (2s, 4H, e-H), 7.27 (2s, 2H, b-H), 7.03 (d, ^3J = 5.8 Hz, 1H, j-H), 4.02 (s, 3H, i-H), 2.59 (s, 9H, [a+f]-H), 1.84 (s, 18H, [c+d]-H) ppm. **^{13}C NMR (THF-d_8, 125 MHz):** Solubility of compound **1** is too low to record. **IR(KBr):** $\tilde{\nu}$ = 3112, 2965, 2916, 2854, 2213, 1817, 1590, 1493, 1335, 1295, 1203, 996, 797, 722 cm^{-1}. **Elemental analysis**: Anal. Calcd. For $C_{61}H_{51}N_5OZn$: C, 78.32; H, 5.50; N, 7.49; Found: C, 78.24; H, 5.33; N, 7.14. **ESI-MS:** *m/z* (%) = 934.3 (100) [**1**+H]$^+$.

Zinc(II)-5-[4-(5-nitro-3-pyridylethynyl)phenyl]-10,15,20-trimesitylporphyrin (2)

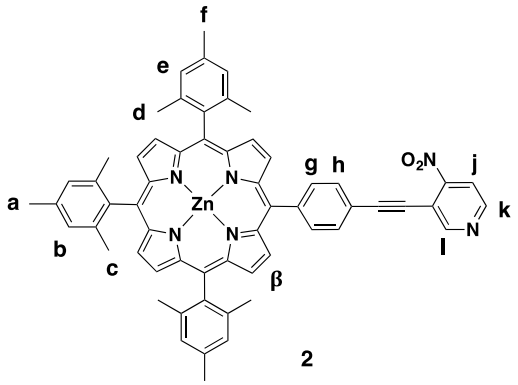

4-Bromo-3-nitropyridine (**9**, 163 mg, 800 μmol) and zinc(II)-5-(4-ethynyl-phenyl)-10,15,20-trimesitylporphyrin (**11**, 150 mg, 200 μmol) were dissolved in dry THF (10.0 mL) and dry *N*,*N*-diisopropylamine (10.0 mL) and the solution was degassed by using two freeze-pump-thaw cycles. Then, $Pd(PPh_3)_4$ (31.0 mg, 30.0 μmol) was added under N_2 atmosphere. One additional freeze-pump-thaw cycle was used for degassing. The mixture was stirred at 70 °C for 14 h (CAUTION: sealed tube). After evaporation of the solvent, the crude product was extracted with CH_2Cl_2 (200 mL), washed by water (100 mL × 3) and dried over anhydrous Na_2SO_4. Then the crude product was purified by size exclusion chromatography using SX-3 biobead with THF affording **2** as a purple solid (201 mg, 176 μmol, 88%). $\boldsymbol{R_f}$ = 0.7 (SiO_2, CH_2Cl_2). **MP:** > 300 °C **^{1}H NMR (THF-d_8, 500 MHz):** δ = 9.16 (s, 1H, l-H), 8.83 (d, ^3J = 5.5 Hz, 1H, k-H), 8.77 (d, ^3J = 4.6 Hz, 2H, β-H), 8.65 (d, ^3J = 4.6 Hz, 2H, β-H), 8.60 (s, 4H, β -H), 8.26 (d, ^3J = 8.0 Hz, 2H, h-H), 8.05 (d, ^3J = 5.5 Hz, 1H, j-H), 7.99 (d, ^3J = 8.0 Hz, 2H, g-H), 7.28 (s, 4H, e-H), 7.27 (s, 2H, b-H), 2.59 (s, 9H, [a+f]-H), 1.85 (s, 18H, [c+d]-H) ppm. **^{13}C NMR ($CDCl_3$, 125 MHz):** Solubility of compound **2** is too low to record. **IR(KBr):** $\tilde{\nu}$ = 3116, 1596, 1534, 1340, 1337, 1204, 1062, 997, 831, 799, 723 cm^{-1}. **Elemental analysis:** Anal. Calcd for $C_{60}H_{48}N_6O_2Zn$: C, 75.82; H, 5.09; N, 8.84; Found: C, 75.74; H, 4.88; N, 8.52. **ESI-MS:** *m/z* (%) = 949.3 (100) $[\mathbf{2}+H]^+$.

Zinc(II)-5-[4-(3-pyridylethynyl)phenyl]-10,15,20-trimesitylporphyrin (3)

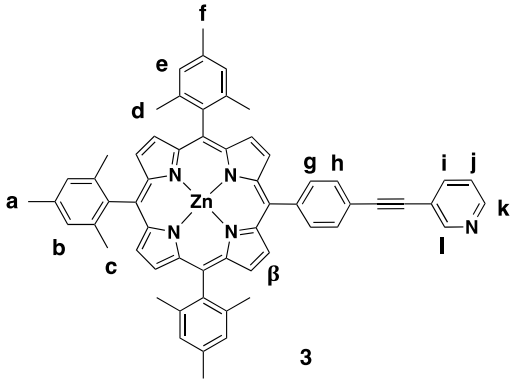

3

3-Bromopyridine (**10**, 163 mg, 800 μmol) and zinc(II)-5-(4-ethynylphenyl)-10,15,20-trimesitylporphyrin (**11**, 150 mg, 200 μmol) were dissolved in dry THF (10.0 mL) and dry *N*,*N*-diisopropylamine (10.0 mL) and the resulting solution was degassed by using two freeze-pump-thaw cycles. Then, $Pd(PPh_3)_4$ (31.0 mg, 30.0 μmol) was added under N_2 atmosphere. One additional freeze-pump-thaw cycle was used for degassing. The mixture was stirred at 70 °C for 14 h (CAUTION: sealed tube). After evaporation of the solvent, the crude product was extracted with CH_2Cl_2 (200 mL), washed by water (100 mL × 3) and dried over anhydrous Na_2SO_4. Then the crude product was purified by size exclusion chromatography using SX-3 biobead with THF affording **3** as a purple solid (147 mg, 162 μmol, 81%). $\boldsymbol{R_f}$ = 0.6 (SiO_2, CH_2Cl_2). **MP:** > 300 °C **^{1}H NMR (THF-d_8, 500 MHz):** δ = 8.79 (s, 1H, l-H), 8.76 (d, ^3J = 4.5 Hz, 2H, β-H), 8.64 (d, ^3J = 4.5 Hz, 2H, β-H), 8.61 (s, 4H, β-H), 8.52 (d, ^3J = 4.7 Hz, 1H, k-H), 8.22 (d, ^3J = 7.9 Hz, 2H, h-H), 7.96 (d, ^3J = 7.8 Hz, 1H, i-H), 7.91 (d, ^3J = 7.9 Hz, 2H, g-H), 7.38 (dd, ^3J = 7.8, 4.7 Hz, 1H, j-H), 7.28 (s, 4H, e-H), 7.27 (s, 2H, b-H), 2.59 (s, 9H, [a+f]-H), 1.84 (s, 18H, [c+d]-H) ppm. **^{13}C NMR ($CDCl_3$, 125 MHz):** Solubility of compound **3** is too low to record. **IR(KBr):** $\tilde{\nu}$ = 2918, 2865, 2844, 2230, 1601, 1521, 1400, 1337, 1204, 1002, 831, 723 cm^{-1}. **Elemental analysis:** Anal. Calcd for $C_{60}H_{49}N_5Zn$: C, 79.59; H, 5.45; N, 7.73; Found: C, 79.34; H, 5.39; N, 7.68. **ESI-MS:** *m/z* (%) = 903.3 (100) $[\mathbf{3}+H]^+$.

6-Bromo-6'-mesityl-2,2'-bipyridine (16)

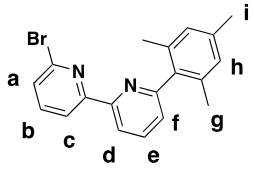

16

Mesitylene-2-boronic acid (**13**, 210 mg, 1.28 mmol) and 6,6'-dibromo-2,2'-bipyridine (**12**, 400 mg, 1.28 mmol) were dissolved in MeOH (24 mL), THF (60 mL) and aqueous K_2CO_3 (2 M, 18 mL) under N_2 atmosphere. The mixture was degassed via two freeze-pump-thaw cycles. Then, $Pd(PPh_3)_4$ (12.3 mg, 10.7 µmol) was added under N_2 atmosphere. After degassing again by freeze-pump-thaw cycle, the reaction mixture was stirred at 90 °C for 12 h (CAUTION: sealed tube). After evaporation of the solvent, the residue was extracted with CH_2Cl_2 (200 mL), washed by water (100 mL × 3) and dried over anhydrous Na_2SO_4. Further purification was achieved by column chromatography on silica gel using 30% CH_2Cl_2 in *n*-hexane furnishing product **16** as a colorless solid (338 mg, 960 µmol, 75%). $\boldsymbol{R_f}$ = 0.2 (SiO_2, 20% CH_2Cl_2 in *n*-hexane). **MP:** 254-255 °C. **^{1}H NMR ($CDCl_3$, 500 MHz):** δ = 8.41 (d, ^3J = 7.8 Hz, 1H, c-H), 8.37 (d, ^3J = 7.8 Hz, 1H, d-H), 7.88 (t, ^3J = 7.8 Hz, 1H, e-H), 7.61 (t, ^3J = 7.8 Hz, 1H, b-H), 7.47 (d, ^3J = 7.8 Hz, 1H, a-H), 7.26 (d, ^3J = 7.5 Hz, 1H, f-H), 6.98 (s, 2H, h-H), 2.36 (s, 3H, i-H), 2.08 (s, 6H, g-H) ppm. **^{13}C NMR ($CDCl_3$, 125 MHz):** δ = 159.3, 157.6, 154.3, 141.4, 139.1, 137.7, 137.6, 137.1, 135.8, 128.4, 127.8, 125.3, 120.1, 119.2, 21.1, 20.3 ppm. **IR(KBr):** $\tilde{\nu}$ = 2919, 1610, 1573, 1546, 1412, 1151, 1121, 1072, 1043, 855, 798, 761, 718, 628 cm^{-1}. **Elemental analysis:** Anal. Calcd for $C_{19}H_{17}BrN_2$: C, 64.60; H, 4.85; N, 7.93. Found: C, 64.54; H, 4.82; N, 7.85. **ESI-MS:** *m/z* (%) = 353.2 (100) [**16**+H]$^+$.

4,4,5,5-Tetramethyl-2-[4-[2-(trimethylsilyl)ethynyl]-2,3,5,6-tetramethylphenyl]-1,3,2-dioxaborolane (17)

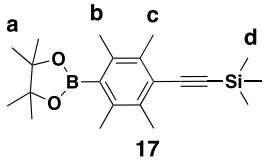

17

1-Iodo-2,3,5,6-tetramethyl-4-[2-(trimethylsilyl)ethynyl]-benzene (**14**, 1.78 g, 5.00 mmol) was dissolved in anhydrous THF (50 mL) at –78 °C. The mixture was treated with 2.5 M *n*-BuLi (2.00 mL, 5.00 mmol) and stirred for 1 h under N_2 atmosphere. Isopropoxyboronic acid pinacol ester (**15**, 2.10 ml, 10.0 mmol) was added, the reaction removed from the cooling bath and warmed to room temperature. Upon reaching room temperature the reaction was quenched by saturated ammonium chloride solution (50 mL) and extracted with CH_2Cl_2 (100 ml). The organic phase was washed with water (100 mL × 3) and dried over anhydrous Na_2SO_4. Further purification was achieved by column chromatography on silica gel using 50% CH_2Cl_2 in *n*-hexane furnishing product **17** as a colorless solid (1.10 g, 3.08 mmol, 80%). $\boldsymbol{R_f}$ = 0.4 (SiO_2, 30% CH_2Cl_2 in *n*-hexane). **MP:** 97-98 °C. **^{1}H NMR ($CDCl_3$, 500 MHz):** δ = 2.35 (s, 6H, b-H), 2.25 (s, 6H, c-H), 1.40 (s, 12H, a-H), 0.26 (s, 9-H, d-H) ppm. **^{13}C NMR ($CDCl_3$, 125 MHz):** δ = 136.1, 135.5, 124.0, 104.5, 101.7, 83.9, 25.1 (2s), 19.7, 17.9, 0.2 ppm. **IR(KBr):** $\tilde{\nu}$ = 2979, 2141, 1413,1344, 1304, 1248, 1215, 1143, 862, 760, 716, 662 cm^{-1}. **Elemental analysis:** Anal. Calcd for $C_{21}H_{33}BO_2Si$: C, 70.77; H, 9.33, Found: C, 70.38; H, 9.61.

6-[4-[2-(Trimethylsilyl)ethynyl]ethynyl-2,3,5,6-tetramethyl]phenyl-6'-(2,4,6-trimethyl)phenyl-2,2'-bipyridine (18)

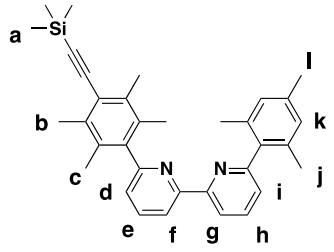

18

6-Bromo-6'-mesityl-2,2'-bipyridine (**16**, 176 mg, 500 μmol) and 4,4,5,5-tetramethyl-2-[4-[2-(trimethylsilyl)ethynyl]-2,3,5,6-tetramethylphenyl]-1,3,2-dioxaborolane (**17**, 180 mg, 505 μmol) were dissolved in THF (60 mL) and aqueous K_2CO_3 (2 M, 18 mL) under N_2 atmosphere. The mixture was degassed by using two freeze-pump-thaw cycles. Then, $Pd(PPh_3)_4$ (5.00 mg, 5.00 μmol) was added under N_2 atmosphere. After degassing again by freeze-pump-thaw cycle, the reaction mixture was stirred at 90 °C for 12 h (CAUTION: sealed tube). After evaporation of the solvent, the crude product was extracted with CH_2Cl_2 (200 mL), washed with water (100 mL × 3)

and dried over anhydrous Na_2SO_4. Further purification was achieved by column chromatography on silica gel using 20% CH_2Cl_2 in *n*-hexane furnishing the product as a colorless solid (71.0 mg, 165 µmol, 85%). $\boldsymbol{R_f}$ = 0.1 (SiO_2, 20% CH_2Cl_2 in *n*-hexane). **MP:** decomposed at 105 °C before melting. **^{1}H NMR ($CDCl_3$, 500 MHz):** δ = 8.40 (dd, ^3J = 7.7 Hz, ^4J = 1.0 Hz, 1H, f-H), 8.35 (dd, ^3J = 7.7 Hz, ^4J = 1.0 Hz, 1H, g-H), 7.81 (t, ^3J = 7.7 Hz, 1H, e/h-H), 7.81 (t, ^3J = 7.7 Hz, 1H, h/e-H), 7.22 (dd, ^3J = 7.7 Hz, ^4J = 1.0 Hz, 1H, i-H), 7.15 (dd, ^3J = 7.7 Hz, ^4J = 1.0 Hz, 1H, d-H), 6.99 (s, 2H, k-H), 2.47 (s, 6H, c-H), 2.36 (s, 3H, l-H), 2.12 (s, 6H, j-H), 1.97 (s, 6H, b-H), 0.30 (s, 9H, a-H) ppm. **^{13}C NMR ($CDCl_3$, 125 MHz):** δ = 160.2, 159.1, 156.3, 156.1, 141.2, 138.0, 137.4, 136.9, 136.9, 136.5, 135.9, 131.7, 128.4, 124.7, 124.6, 123.2, 119.3, 109.9, 104.3, 101.9, 21.1, 20.4, 18.4, 17.6, 0.2 ppm. **IR(KBr):** $\tilde{\nu}$ = 3169, 3120, 2398, 1697, 1639, 1623, 1580, 1431, 1157, 977, 965, 946, 722 cm^{-1}. **Elemental analysis:** Anal. Calcd for $C_{34}H_{38}N_2Si$: C, 81.22; H, 7.62; N, 5.57. Found: C, 81.12; H, 7.73; N, 5.52. **ESI-MS:** *m/z* (%) = 503.3 (100) [**18**+H]$^+$.

6-(4-Ethynyl-2,3,5,6-tetramethyl)phenyl-6'-(2,4,6-trimethyl)phenyl-2,2'-bipyridine (19)

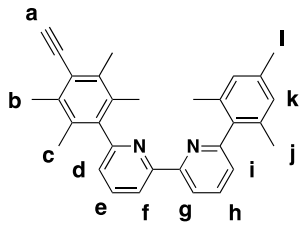

19

6-[4-[2-(Trimethylsilyl)ethynyl]ethynyl-2,3,5,6-tetramethyl]phenyl-6'-(2,4,6-trimethyl)phenyl-2,2'-bipyridine (**18**, 50 mg, 99.6 µmol) was dissolved in a solution of MeOH (20 mL) and THF (10 mL). K_2CO_3 (1.00 g, 7.23 mmol) was added. The resultant suspension was stirred at room temperature overnight. The mixture was filtered and the solvent was removed at room temperature. The crude product was extracted with CH_2Cl_2 (200 mL), washed by water (100 mL × 3) and dried over anhydrous Na_2SO_4 without further purification yielding a colorless solid (40.7 mg, 94.6 µmol, 95%). $\boldsymbol{R_f}$ = 0.1 (SiO_2, 20% CH_2Cl_2 in *n*-hexane). **MP:** 246-247 °C **^{1}H NMR (CD_2Cl_2, 500 MHz):** δ = 8.40 (dd, ^3J = 7.8 Hz, ^4J = 1.0 Hz, 1H, f-H), 8.33 (dd, ^3J = 7.8 Hz, ^4J = 1.0 Hz, 1H, g-H), 7.86 (t, ^3J = 7.8 Hz, 1H, e-H), 7.84 (t, ^3J = 7.8 Hz, 1H, h-H),

7.23 (dd, ^3J = 7.8 Hz, ^4J = 1.0 Hz, 1H, d-H), 7.18 (dd, ^3J = 7.8 Hz, ^4J = 1.0 Hz, 1H, i-H), 6.98 (s, 2H, k-H), 3.60 (s, 1H, a-H), 2.49 (s, 6H, c-H), 2.35 (s, 3H, l-H), 2.08 (s, 6H, j-H), 1.96 (s, 6H, b-H) ppm. **^{13}C NMR ($CDCl_3$, 125 MHz):** δ = 160.4, 159.5, 156.5, 156.3, 142.0, 138.4, 137.8, 137.4, 137.3, 137.1, 136.1, 132.2, 128.6, 125.3, 124.9, 122.3, 119.4, 119.2, 85.1, 82.8, 21.2, 20.4, 18.5, 17.6 ppm. **IR(KBr):** $\tilde{\nu}$ = 3571, 3241, 3170, 3121, 1710, 1697, 1639, 1623, 1588, 1226, 946, 874, 858 cm^{-1}. **Elemental analysis:** Anal. Calcd for $C_{31}H_{30}N_2$: C, 86.47; H, 7.02; N, 6.51. Found: C, 86.39; H, 6.95; N, 6.43. **ESI-MS:** *m/z* (%) = 431.2 (100) [**19**+H]$^+$.

Compound 4

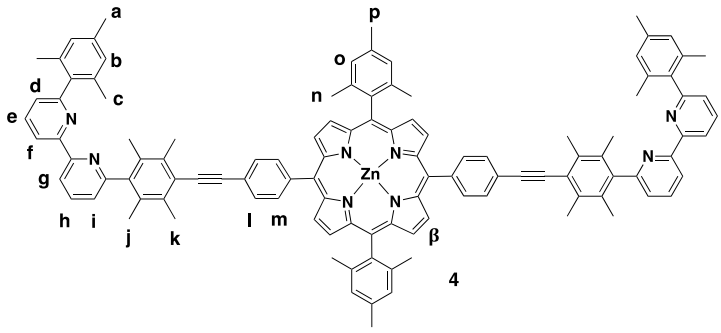

In a 50-mL sealed tube, a solution of zinc(II) *meso*-5,15-bis(2,4,6-trimethyl-phenyl)-10,20-bis(4-iodophenyl)porphyrin (**20**, 100 mg, 98.6 μmol) and 6-(4-ethynyl-2,3,5,6-tetramethyl)phenyl-6'-(2,4,6-trimethyl)phenyl-2,2'-bipyridine (**19**, 180 mg, 394 μmol) in dry THF (10.0 mL) and dry *N*,*N*-diisopropylamine (10.0 mL) was degassed by using two freeze-pump-thaw cycles. Then, $Pd(PPh_3)_4$ (10.0 mg, 10.0 μmol) was added under N_2 atmosphere. One additional freeze-pump-thaw cycle was used for degassing. The mixture was stirred at 75 °C for 14 h. After evaporation of the solvent, the crude product was extracted with CH_2Cl_2 (200 mL), washed by water (100 mL × 3) and dried over anhydrous Na_2SO_4. Thereafter the crude product was purified by size exclusion chromatography using SX-3 biobead with THF affording a purple solid (128 mg, 78.9 μmol, 80%). $\boldsymbol{R}_\mathbf{f}$ = 0.5 (SiO_2, CH_2Cl_2). **MP:** > 300 °C **^{1}H NMR ($CDCl_3$, 500 MHz):** δ = 8.96 (d, ^3J = 4.6 Hz, 4H, β-H), 8.82 (d, ^3J = 4.6 Hz, 4H, β-H), 8.45 (d, ^3J = 7.9 Hz, 2H, f/g-H), 8.42 (d, ^3J = 7.9 Hz, 2H, g/f-H), 8.27 (d, ^3J = 8.0 Hz, 4H, l-H), 7.98 (d, ^3J = 8.0 Hz, 4H, m-H), 7.87 (t, J = 7.9 Hz, 2H, e/h-H), 7.84 (t, J =7.9 Hz, 2H, h/e -H), 7.31 (s, 4H, o-H), 7.26 (d, ^3J = 7.9 Hz, 4H, [d+i]-H), 7.00 (s, 4H, b-H), 2.72 (s, 12H, k-H), 2.65 (s, 6H, p-H), 2.37 (s, 6H, a-H), 2.15 (s, 12H, c-H), 2.08 (s, 12H,

j-H), 1.86 (s, 12H, n-H) ppm. **^{13}C NMR ($CDCl_3$, 125 MHz):** δ = 160.2, 159.1, 156.3, 156.1, 150.0, 149.9, 142.6, 141.3, 139.2, 138.9, 138.0, 137.54, 137.47, 137.02, 136.96, 136.4, 135.9, 134.5, 132.2 (2), 131.9, 131.0, 129.6, 128.4, 127.7, 124.8, 124.6, 123.3, 123.2, 119.7, 119.5, 119.4, 97.1, 89.8, 21.7, 21.5, 21.1, 20.4, 18.7, 17.7 ppm. **IR(KBr):** $\tilde{\nu}$ = 3200, 2973, 2630, 2416, 1567, 1453, 1419, 1402, 1268, 1000, 812, 800 cm^{-1}. **Elemental analysis:** Anal. Calcd for $C_{112}H_{96}N_8Zn$: C, 83.07; H, 5.98; N, 6.92. Found: C, 82.74; H, 5.59; N, 6.57. **ESI-MS:** *m/z* (%) = 810.9 (100) [**4**+2H]$^{2+}$.

1.3. Synthesis and Characterization of Complexes

Pre-Rotor Complex **ROT-1a**

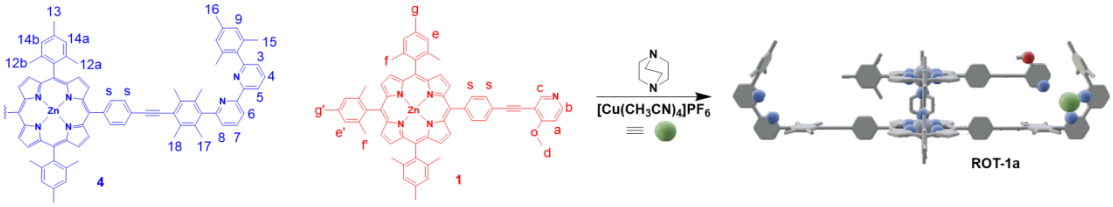

In an NMR tube, stator **4** (1.58 mg, 976 nmol) was mixed with 1 equiv of $[Cu(CH_3CN)_4]PF_6$ (364 µg, 976 nmol) and dissolved in 100 µL of CD_2Cl_2, followed by addition of rotator **1** (913 µg, 976 nmol), DABCO (109 µg, 976 nmol) and further 400 µL of CD_2Cl_2. After subsequent sonication for 10 min the purple complex was obtained in quantitative yield. **Mp** > 250 °C. **^{1}H NMR (CD_2Cl_2, 500 MHz):** δ = 8.59 (d, ^3J = 4.5 Hz, 2H, β(**4**)-H), 8.58 (d, ^3J = 4.5 Hz, 2H, β(**4**)-H), 8.53 (d, ^3J = 4.5 Hz, 4H, β(**4**)-H), 8.47 (d, ^3J = 7.9 Hz, 2H, [5u+6u]-H), 8.38 (d, ^3J = 4.5 Hz, 4H, β(**1**)-H), 8.35 (m, 4H, [4c+5c+6c+7c]-H), 8.32 (d, ^3J = 4.5 Hz, 2H, β(**1**)-H), 8.27 (d, ^3J = 4.5 Hz, 2H, β(**1**)-H), 7.93 (s, 7H, [s+a]-H), 7.90 (t, ^3J = 7.9 Hz, 2H, [4u+7u]-H), 7.73 (d, ^3J = 7.9 Hz, 1H, [3c/8c]-H), 7.72 (d, ^3J = 7.9 Hz, 1H, [8c/3c+c]-H), 7.30 (d, ^3J = 7.9 Hz, 1H, [3u/8u]-H), 7.28 (d, ^3J = 7.9 Hz, 1H, [8u/3u]-H), 7.23 (brs, 16H, [e+e'+s+14a+14b]-H), 7.01 (s, 2H, 9u-H), 6.92 (s, 2H, 9c-H), 6.65 (s, 1H, b-H), 4.10 (s, 3H, d-H), 2.77 (s, 6H, 17u-H), 2.61 (s, 6H, 17c-H), 2.59 (s, 6H, 13-H), 2.58 (s, 9H, [g+g']-H), 2.38 (s, 3H, 16u-H), 2.33 (s, 3H, 16c-H), 2.12 (s, 6H, 15u-H), 2.10 (s, 12H, [18u+15c]-H), 2.06 (s, 6H, 18c-H), 1.81 (brs, 12H, [12a+12b]-H), 1.53 (brs, 6H, f'-H), 1.26 (brs, 12H, f-H), –[4.42-4.49] (m, 6H, CH_2, DABCO-H), –[4.51-4.56] (m, 6H, CH_2, DABCO-H) ppm. **Elemental**

analysis: Anal. Calcd. for $C_{179}H_{159}OCuN_{15}Zn_2$•$2.5CH_2Cl_2$: C, 74.07; H, 5.62; N, 7.14; Found: C, 74.24; H, 5.57; N, 7.10. **ESI-MS**: *m/z* (%) = 1309.5 (100) $[Cu(\mathbf{1})(\mathbf{4})(H)]^{2+}$.

Nanorotor **ROT-1a'**

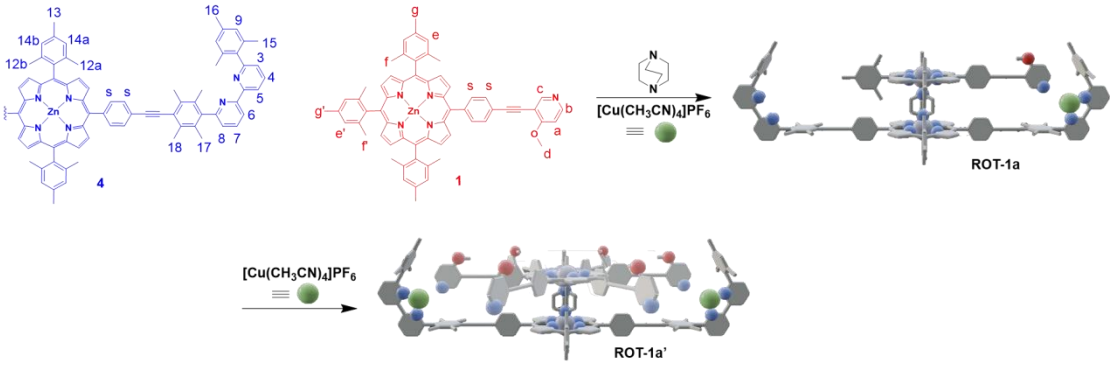

One equiv of $[Cu(CH_3CN)_4]PF_6$ (364 μg, 976 nmol) was added to complex **ROT-1a** (2.97 mg, 976 nmol). After subsequent sonication for 10 min the purple complex was obtained in quantitative yield. **Mp** > 250 °C. **^{1}H NMR (CD_2Cl_2, 500 MHz):** δ = 8.58 (brs, 2H, β(**4**)-H), 8.54 (d, ^3J = 4.5 Hz, 4H, β(**4**)-H), 8.40 (d, ^3J = 4.5 Hz, 2H, β(**4**)-H), 8.38 (d, ^3J = 4.5 Hz, 4H, β(**1**)-H), 8.35 (m, 8H, [4+5+6+7]-H), 8.32 (d, ^3J = 4.5 Hz, 2H, β(**1**)-H), 8.30 (d, ^3J = 4.5 Hz, 2H, β(**1**)-H), 7.94 (d, ^3J = 6.4 Hz, 3H, [s+a]-H), 7.89 (d, ^3J = 7.5 Hz, 4H, s-H), 7.72 (d, ^3J = 7.9 Hz, 3H, [3/8+c]-H), 7.69 (d, ^3J = 7.9 Hz, 2H, [8/3]-H), 7.21 (brs, 16H, [e+e'+s+14a+14b]-H), 6.97 (s, 4H, 9-H), 6.66 (s, 1H, b-H), 4.10 (s, 3H, d-H), 2.67 (s, 12H, 17-H), 2.59 (s, 9H, [g+g']-H), 2.58 (s, 6H, 13-H), 2.34 (s, 6H, 16-H), 2.08 (s, 12H, 15-H), 2.04 (s, 12H, 18-H), 1.81 (brs, 12H, [12a+12b]-H), (1.74 (brs, 6H, [12a/12b]-H), 1.66 (brs, 6H, [12b/12a]-H), 0 °C), 1.53 (brs, 6H, f'-H), 1.26 (brs, 12H, f-H), –4.48 (brs, 6H, CH_2, DABCO-H), –4.53 (brs, 6H, CH_2, DABCO-H) ppm. **ESI-MS**: *m/z* (%) = 1341.0 (100) $[Cu_2(\mathbf{1})(\mathbf{4})]^{2+}$.

Pre-Rotor Complex **ROT-1b**

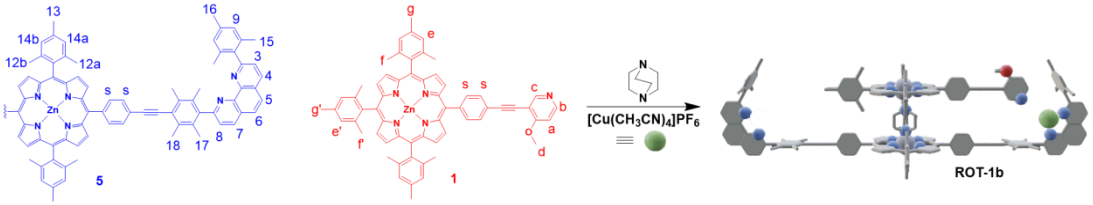

In an NMR tube, stator **5** (1.44 mg, 864 nmol) was mixed with 1 equiv of $[Cu(CH_3CN)_4]PF_6$ (322 µg, 864 nmol) and dissolved in 100 µL of CD_2Cl_2, followed by addition of rotator **1** (808 µg, 864 nmol), DABCO (96.9 µg, 864 nmol) and 400 µL more CD_2Cl_2. After subsequent sonication for 10 min the purple complex was obtained in quantitative yield. **Mp** > 250 °C. **^{1}H NMR (CD_2Cl_2, 500 MHz):** δ = 8.78 (d, ^3J = 8.0 Hz, 1H, [4c/7c]-H), 8.76 (d, ^3J = 8.0 Hz, 1H, [7c/4c]-H), 8.61 (d, ^3J = 4.5 Hz, 2H, β(**5**)-H), 8.56 (d, ^3J = 4.5 Hz, 4H, β(**5**)-H), 8.53 (d, ^3J = 4.5 Hz, 2H, β(**5**)-H), 8.42 (d, ^3J = 8.0 Hz, 2H, [4u+7u]-H), 8.38 (s, 1H, [5c/6c]-H), 8.37 (s, 1H, [6c/5c]-H), 8.34 (d, ^3J = 4.5 Hz, 4H, β(**1**)-H), 8.31 (d, ^3J = 4.5 Hz, 2H, β(**1**)-H), 8.27 (d, ^3J = 4.5 Hz, 2H, β(**1**)-H), 8.24 (s, 2H, s-H), 8.01 (d, ^3J = 8.0 Hz, 1H, [3c/8c]-H), 7.99 (d, ^3J = 8.0 Hz, 1H, [8c/3c]-H), 7.94 (brs, 7H, [s+a]-H), 7.89 (s, 1H, [5u/6u]-H), 7.88 (s, 1H, [6u/5u]-H), 7.63 (d, ^3J = 8.0 Hz, 1H, [3u/8u]-H), 7.61 (d, ^3J = 8.0 Hz, 2H, [8u/3u+c]-H), 7.22 (brs, 16H, [e+e'+s+14a+14b]-H), 7.01 (s, 2H, 9c-H), 6.96 (s, 2H, 9u-H), 6.59 (s, 1H, b-H), 4.10 (s, 3H, d-H), 2.74 (s, 6H, 17u-H), 2.59 (s, 6H, 17c-H), 2.58 (s, 9H, [g+g']-H), 2.57 (s, 6H, 13-H), 2.40 (s, 3H, 16u-H), 2.38 (s, 3H, 16c-H), 2.13 (s, 6H, 15u-H), 2.10 (s, 12H, [15c+18u]-H), 2.05 (s, 6H, 18c-H), 1.83 (brs, 6H, [12a/12b]-H), 1.70 (brs, 6H, [12b/12a]-H), 1.49 (brs, 6H, f'-H), 1.26 (brs, 12H, f-H), –4.47 (brs, 6H, CH_2, DABCO-H), –4.55 (brs, 6H, CH_2, DABCO-H) ppm. **Elemental analysis:** Anal. Calcd. for $C_{183}H_{159}OCuN_{15}Zn_2$•$0.5CH_2Cl_2$: C, 78.12; H, 5.72; N, 7.45; Found: C, 78.34; H, 5.38; N, 7.41. **ESI-MS**: *m/z* (%) = 1333.5 (100) $[Cu(\mathbf{1})(\mathbf{5})(H)]^{2+}$.

Nanorotor **ROT-1b'**

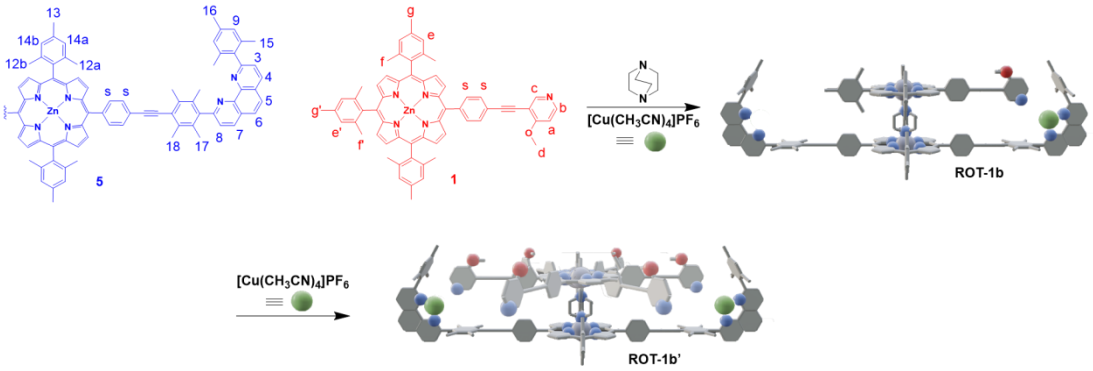

One equiv of $[Cu(CH_3CN)_4]PF_6$ (332 µg, 864 nmol) was added to complex **ROT-1b** (2.67 mg, 864 nmol). After subsequent sonication for 10 min the purple complex was obtained in quantitative yield. **Mp** > 250 °C. **^{1}H NMR (CD_2Cl_2, 500 MHz):** δ = 8.78 (d, ^3J = 8.0 Hz, 2H, [4/7]-H), 8.75 (d, ^3J = 8.0 Hz, 2H, [7/4]-H), 8.56 (d, ^3J = 4.5 Hz, 8H, β(**5**)-H), 8.36 (d, ^3J = 4.5 Hz, 8H, β(**1**)-H), 8.30 (s, 2H, [5/6]-H), 8.28 (s, 2H, [6/5]-H), 8.19 (s, 2H, s-H), 8.01 (d, ^3J = 8.0 Hz, 2H, [3/8]-H), 7.98 (d, ^3J = 8.0 Hz, 2H, [8/3]-H), 7.93 (s, 5H, [s+a]-H), 7.52 (brs, 1H, c-H), 7.30 (s, 2H, s-H), 7.22 (brs, 14H, [e+e'+s+14a+14b]-H), 7.04 (s, 4H, 9-H), 6.60 (s, 1H, b-H), 4.09 (s, 3H, d-H), 2.75 (s, 12H, 17-H), 2.58 (s, 9H, [g+g']-H), 2.57 (s, 6H, 13-H), 2.40 (s, 12H, 16-H), 2.11 (s, 12H, 18-H), 2.07 (s, 12H, 15-H), 1.82 (brs, 6H, [12a/12b]-H), 1.71 (brs, 6H, [12b/12a]-H), (1.76 (brs, 6H, [12a/12b]-H), 1.66 (brs, 6H, [12b/12a]-H), 0 °C), 1.50 (brs, 6H, f'-H), 1.27 (brs, 12H, f-H), –4.47 (brs, 6H, CH_2, DABCO-H), –4.54 (brs, 6H, CH_2, DABCO-H) ppm. **ESI-MS**: *m/z* (%) = 1365.0 (100) $[Cu_2(\mathbf{1})(\mathbf{5})]^{2+}$.

Pre-Rotor Complex **ROT-2**

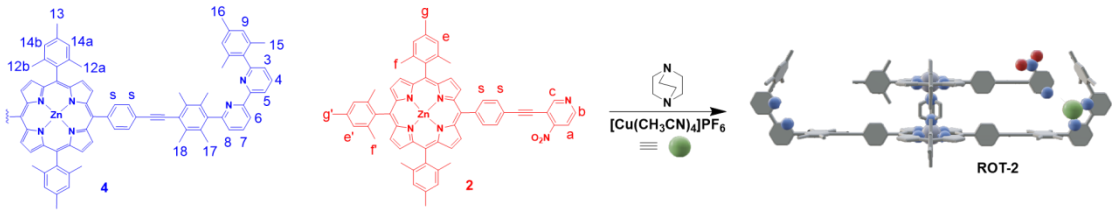

In an NMR tube, stator **4** (1.51 mg, 932 nmol) was mixed with 1 equiv of $[Cu(CH_3CN)_4]PF_6$ (348 µg, 932 nmol) and dissolved in 100 µL of CD_2Cl_2, followed by addition of rotator **2** (886 µg, 932 nmol), DABCO (105 µg, 932 nmol) and 400 µL more CD_2Cl_2. After subsequent sonication for 10 min the purple complex was obtained in quantitative yield. **Mp** > 250 °C. **^{1}H NMR (CD_2Cl_2, 500 MHz):** δ = 8.62 (d, ^3J = 4.5 Hz, 2H, β(**4**)-H), 8.58 (d, ^3J = 4.5 Hz, 4H, β(**4**)-H), 8.64 (d, ^3J = 4.5 Hz, 2H, β(**4**)-H), 8.36 (d, ^3J = 7.9 Hz, 1H, [5u/6u]-H), 8.42 (d, ^3J = 7.9 Hz, 1H, [6u/5u]-H), 8.39 (d, ^3J = 4.5 Hz, 4H, β(**2**)-H), 8.36 (m, 4H, [4c+5c+6c+7c]-H), 8.34 (d, ^3J = 4.5 Hz, 2H, β(**2**)-H), 8.30 (d, ^3J = 4.5 Hz, 2H, β(**2**)-H), 8.00 (d, ^3J = 8.0 Hz, 3H, [s+c]-H), 7.94 (d, ^3J = 7.9 Hz, 1H, [4u/7u]-H), 7.91 (d, ^3J = 7.9 Hz, 1H, [7u/4u]-H), 7.89 (d, ^3J = 8.0 Hz, 6H, s-H), 7.74 (m, 2H, [3c+8c]-H), 7.29 (d, ^3J = 7.9 Hz, 1H, [3u/8u]-H), 7.28(d, ^3J = 7.9 Hz, 1H, [8u/3u]-H), 7.22 (brs, 16H, [e+e'+s+14a+14b]-H), 7.01 (s, 3H, [9u+b]-H), 6.90 (s, 2H, 9c-H), 2.76 (s, 6H, 17u-H), 2.60 (s, 6H, 17c-H), 2.59 (s, 9H, [g+g']-H), 2.58 (s, 6H, 13-H), 2.37 (s, 3H, 16u-H), 2.27 (s, 3H, 16c-H), 2.12 (s, 6H, 15u-H), 2.09 (s, 6H, 15c-H), 2.07 (s, 6H, 18u-H), 2.02 (s, 6H, 18c-H), 1.81 (brs, 12H, [12a+12b]-H), 1.51 (brs, 6H, f'-H), 1.26 (brs, 12H, f-H), –4.27 (brs, 12H, CH_2, DABCO-H) ppm. **Elemental analysis:** Anal. Calcd. for $C_{178}H_{156}CuN_{16}O_2Zn_2$•$2CH_2Cl_2$: C, 74.15; H, 5.53; N, 7.69; Found: C, 74.12; H, 5.46; N, 7.68. **ESI-MS**: *m/z* (%) = 1317.0 (100) $[Cu(\mathbf{2})(\mathbf{4})(H)]^{2+}$.

Nanorotor **ROT-2'**

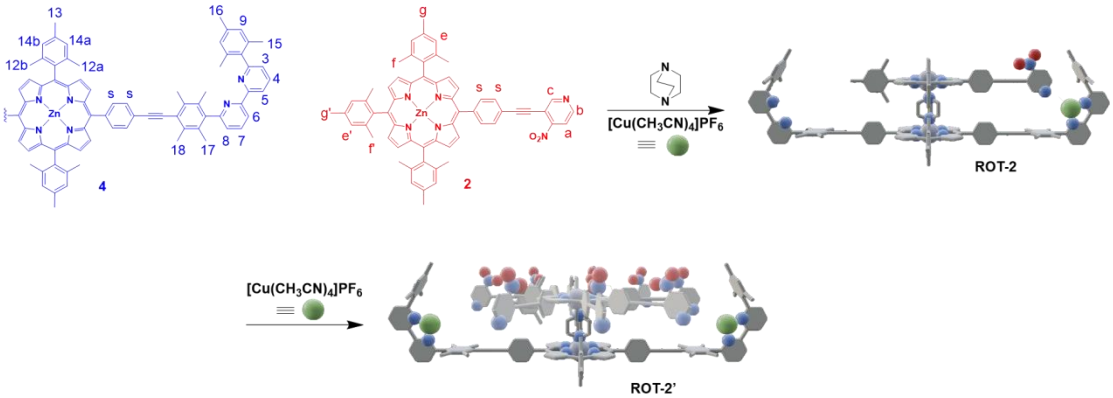

One equiv of $[Cu(CH_3CN)_4]PF_6$ (348 µg, 932 nmol) was added to complex **ROT-2** (2.85 mg, 932 nmol). After subsequent sonication for 10 min the purple complex was obtained in quantitative yield. **Mp** > 250 °C. **^{1}H NMR (CD_2Cl_2, 600 MHz):** δ = 8.58 (brs, 8H, β(**4**)-H), 8.41 (d, ^3J = 4.5 Hz, 2H, β(**2**)-H), 8.40 (d, ^3J = 4.5 Hz, 7H, [β(**2**)+a]-H), 8.32 (m, 8H, [4+5+6+7]-H), 7.99 (d, ^3J = 8.0 Hz, 3H, [s+c]-H), 7.88 (d, ^3J = 8.0 Hz, 6H, s-H), 7.72 (d, ^3J = 7.9 Hz, 2H, [3/8]-H), 7.69 (d, ^3J = 7.9 Hz, 2H, [8/3]-H), 7.22 (brs, 17H, [e+e'+14a+14b+s+b]-H), 6.95 (s, 4H, 9-H), 2.67 (s, 12H, 17-H), 2.59 (s, 9H, [g+g']-H), 2.58 (s, 6H, 13-H), 2.32, (s, 6H, 16-H), 2.06 (s, 12H, 15-H), 2.00 (s, 12H, 18-H), 1.81 (brs, 12H, [12a+12b]-H), (1.80 (brs, 6H, [12a/12b]-H), 1.74 (brs, 6H, [12b/12a]-H), 0 °C), 1.51 (brs, 6H, f'-H), 1.26 (brs, 12H, f-H), –4.35 (brs, 12H, CH_2, DABCO-H) ppm. **ESI-MS**: *m/z* (%) = 1348.5 (100) $[Cu_2(\mathbf{2})(\mathbf{4})]^{2+}$.

Pre-Rotor Complex **ROT-3**

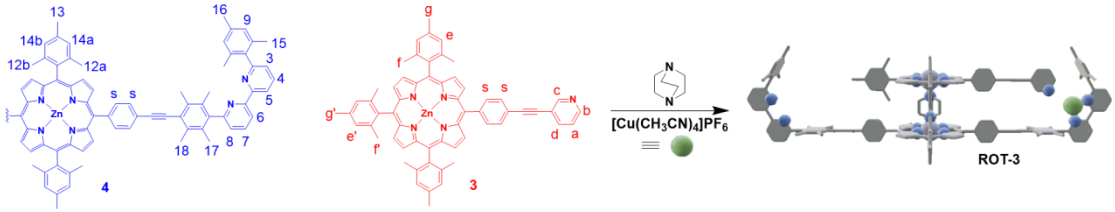

In an NMR tube, stator **4** (1.47 mg, 908 nmol) was mixed with 1 equiv of $[Cu(CH_3CN)_4]PF_6$ (338 µg, 908 nmol) and dissolved in 100 µL of CD_2Cl_2, followed by addition of rotator **3** (822 µg, 908 nmol), DABCO (102 µg, 908 nmol) and 400 µL more CD_2Cl_2. After subsequent sonication for 10 min the purple complex was obtained in quantitative yield. **Mp** > 250 °C. **^{1}H NMR (CD_2Cl_2, 500 MHz):** δ = 8.60 (brs, 2H, β(**4**)-H), 8.58 (d, ^3J = 4.5 Hz, 4H, β(**4**)-H), 8.53 (brs, 2H, β(**4**)-H), 8.46 (d, ^3J = 7.9 Hz, 2H, [5u+6u]-H), 8.36 (d, ^3J = 4.4 Hz, 4H, β(**3**)-H), 8.35 (brs, 4H, [4c+5c+6c+7c]-H), 8.31 (d, ^3J = 4.4 Hz, 2H, β(**3**)-H), 8.27 (d, ^3J = 4.4 Hz, 2H, β(**3**)-H), 8.09 (d, ^3J = 7.3 Hz, 1H, d-H), 7.94 (d, ^3J = 8.0 Hz, 3H, [s+a]-H), 7.90 (brs, 6H, [4u+7u+s]-H), 7.73 (brs, 2H, [3c+8c]-H), 7.51 (s, 1H, c-H), 7.28 (d, ^3J = 7.9 Hz, 1H, [3u/8u]-H), 7.26 (d, ^3J = 7.9 Hz, 1H, [8u/3u]-H), 7.21 (m, 17H, [e+e'+14a+14b+s+b]-H), 7.01 (s, 2H, 9u-H), 6.86 (s, 2H, 9c-H), 2.76 (s, 6H, 17u-H), 2.61 (s, 6H, 17c-H), 2.59 (s, 6H, 13-H), 2.58 (s, 9H, [g+g']-H), 2.37 (s, 3H, 16u-H), 2.26 (s, 3H, 16c-H), 2.11 (s, 6H, 15u-H), 2.09 (s, 6H, 15c-H), 2.06 (s, 6H, 18u-H), 2.04 (s, 6H, 18c-H), 1.81 (brs, 12H, [12a+12b]-H), 1.50 (brs, 6H, f'-H), 1.26 (brs, 12H, f-H), –4.48 (brs, 6H, CH_2, DABCO-H), –4.55 (brs, 6H, CH_2, DABCO-H) ppm. **Elemental analysis:** Anal. Calcd for $C_{178}H_{157}CuN_{15}Zn_2$•$4CH_2Cl_2$: C, 71.90; H, 5.47; N, 6.91; Found: C, 72.05; H, 5.36; N, 6.87. **ESI-MS**: *m/z* (%) = 1294.5 (100) $[Cu(\mathbf{3})(\mathbf{4})(H)]^{2+}$.

Nanorotor **ROT-3'**

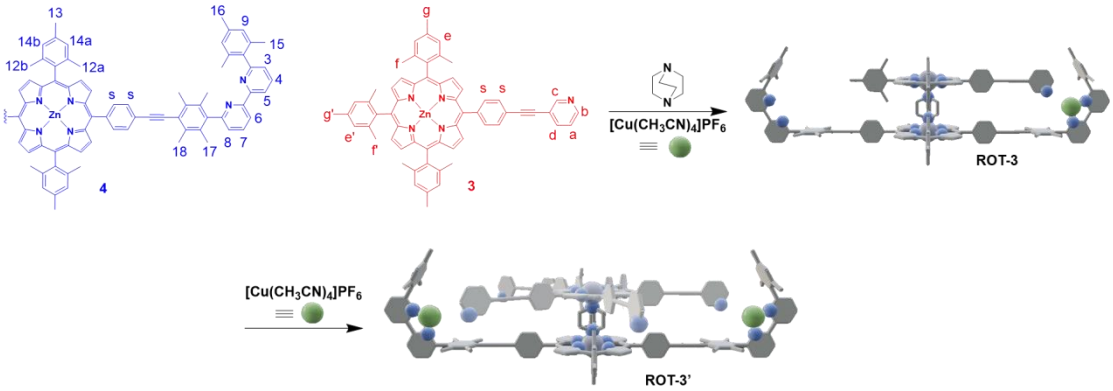

One equiv of $[Cu(CH_3CN)_4]PF_6$ (338 µg, 908 nmol) was added to complex **ROT-3** (2.73 mg, 908 nmol). After subsequent sonication for 10 min the purple complex was obtained in quantitative yield. **Mp** > 250 °C. **^{1}H NMR (CD_2Cl_2, 600 MHz):** δ = 8.58 (d, ^3J = 4.5 Hz, 2H, β(**4**)-H), 8.55 (brs, 4H, β(**4**)-H), 8.41 (d, ^3J = 4.5 Hz, 2H, β(**4**)-H), 8.36 (d, ^3J = 4.5 Hz, 4H, β(**3**)-H), 8.33 (m, 8H, [4+5+6+7]-H), 8.29 (d, ^3J = 4.5 Hz, 2H, β(**3**)-H), 8.26 (d, ^3J = 4.5 Hz, 2H, β(**3**)-H), 8.08 (d, ^3J = 7.3 Hz, 1H, d-H), 7.94 (brs, 3H, [s+a]-H), 7.88 (brs, 4H, s-H), 7.71 (d, ^3J = 7.9 Hz, 2H, [3/8]-H), 7.68 (d, ^3J = 7.9 Hz, 2H, [8/3]-H), 7.53 (s, 1H, c-H), 7.24 (s, 2H, s-H), 7.21 (brs, 15H, [e+e'+14a+14b+s+b]-H), 6.93 (s, 4H, 9-H), 2.66 (s, 12H, 17-H), 2.59 (s, 6H, 13-H), 2.58 (s, 9H, [g+g']-H), 2.31 (s, 6H, 16-H), 2.07 (s, 12H, 15-H), 2.02 (s, 12H, 18-H), 1.81 (brs, 12H, [12a+12b]-H), (1.75 (brs, 6H, [12a/12b]-H), 1.66 (brs, 6H, [12b/12a]-H), 0 °C), 1.49 (brs, 6H, f'-H), 1.26 (brs, 12H, f-H), –4.47 (brs, 6H, CH_2, DABCO-H), –4.54 (brs, 6H, CH_2, DABCO-H) ppm. **ESI-MS**: *m/z* (%) = 1326.0 (100) $[Cu_2(\mathbf{3})(\mathbf{4})]^{2+}$.

2. NMR Spectra: ^{1}H, ^{13}C, ^{1}H-^{1}H COSY

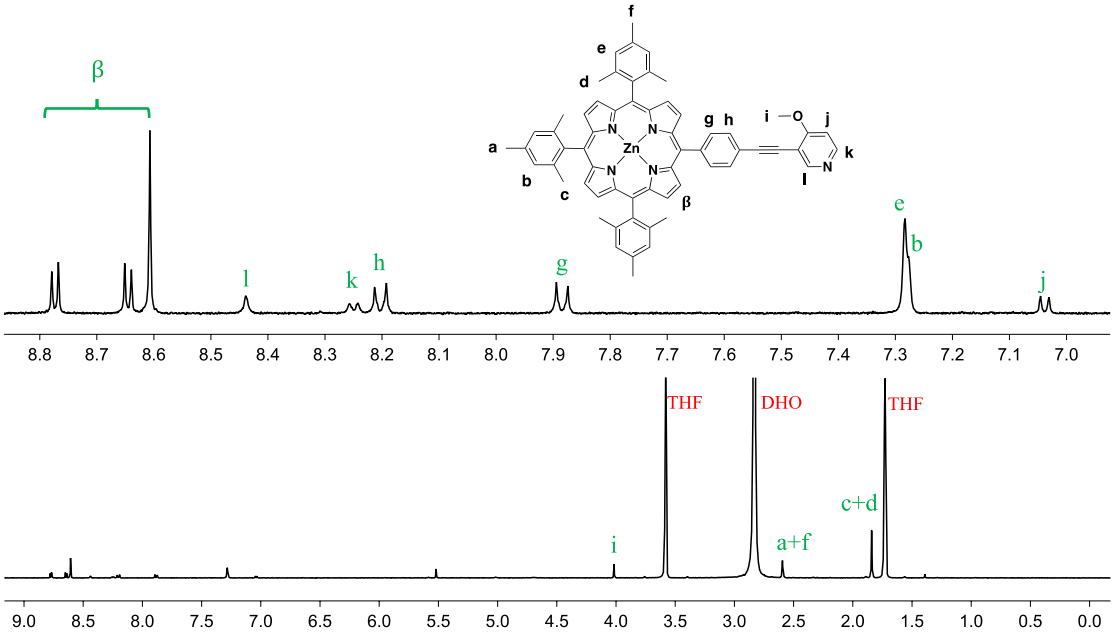

Figure S1. ^{1}H NMR of compound **1** in the THF-d_8 (500 MHz, 298 K)

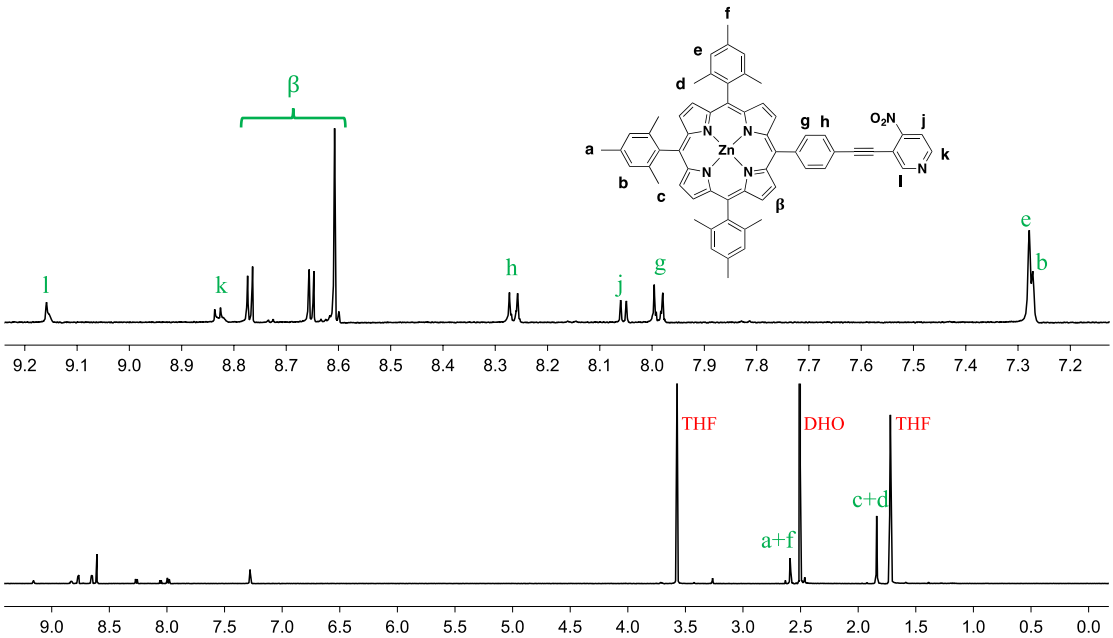

Figure S2. ^{1}H NMR of compound **2** in the THF-d_8 (500 MHz, 298 K)

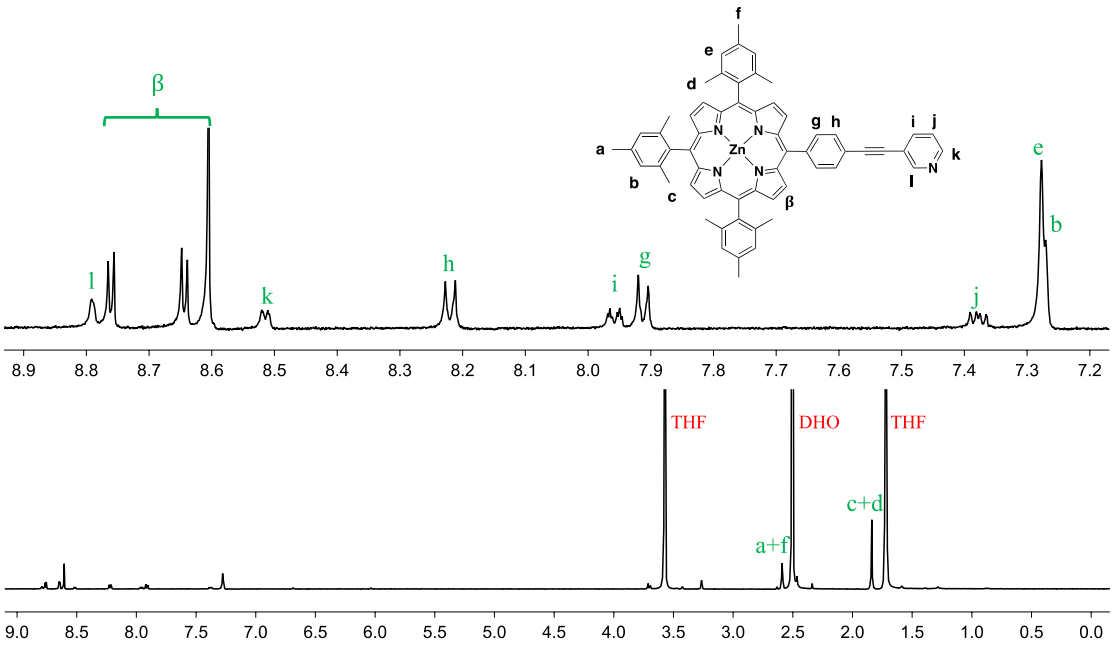

Figure S3. ^{1}H NMR of compound **3** in the THF-d_8 (500 MHz, 298K)

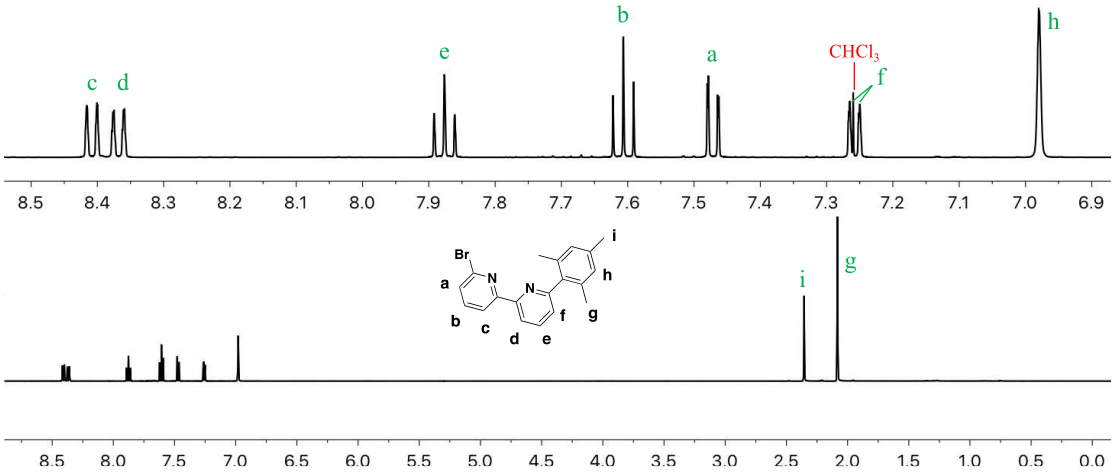

Figure S4. ^{1}H NMR of compound **16** in the $CDCl_3$ (500 MHz, 298 K)

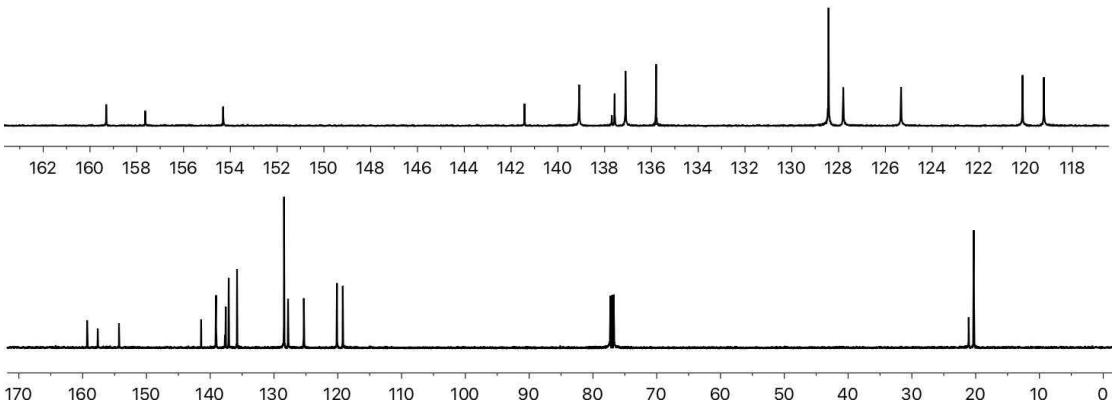

Figure S5. ^{13}C NMR of compound **16** in the $CDCl_3$ (125 MHz, 298 K)

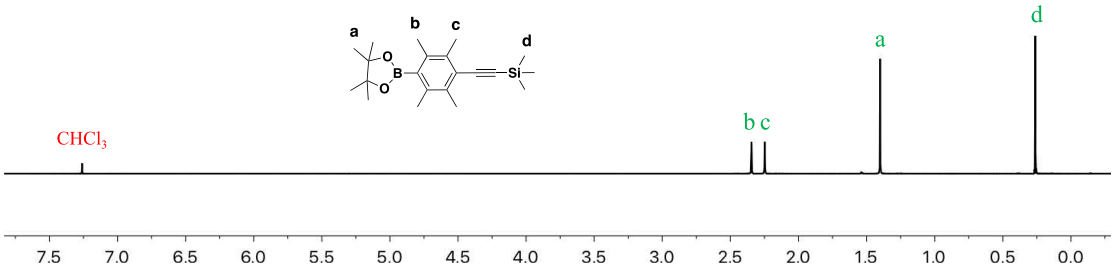

Figure S6. ^{1}H NMR of compound **17** in the $CDCl_3$ (500 MHz, 298 K)

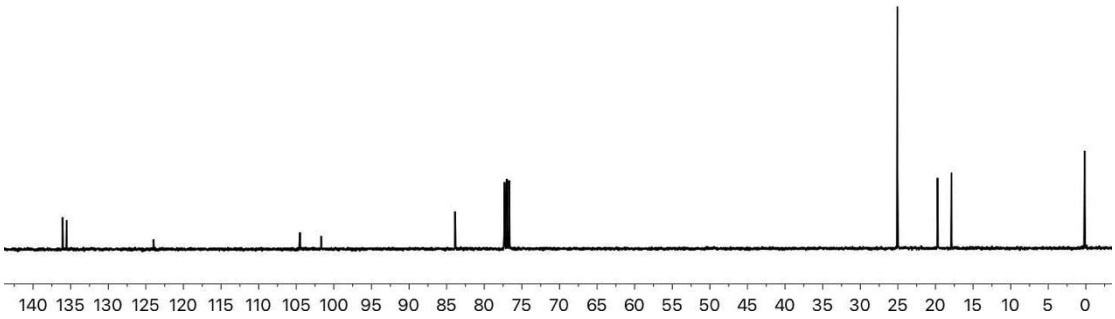

Figure S7. ^{13}C NMR of compound **17** in the $CDCl_3$ (125 MHz, 298 K)

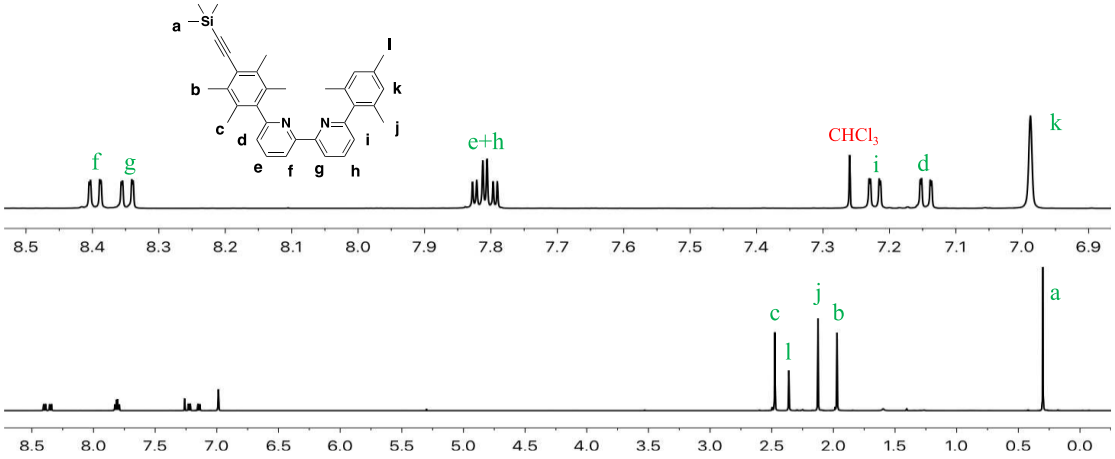

Figure S8. ^{1}H NMR of compound **18** in the $CDCl_3$ (500 MHz, 298 K)

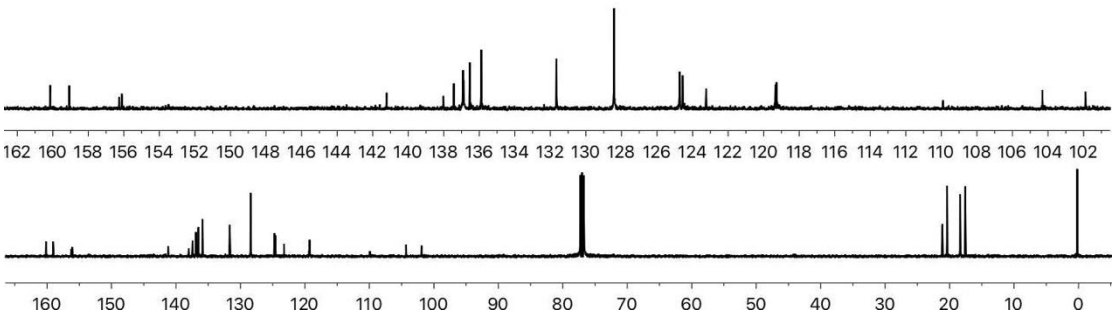

Figure S9. ^{13}C NMR of compound **18** in the $CDCl_3$ (125 MHz, 298 K)

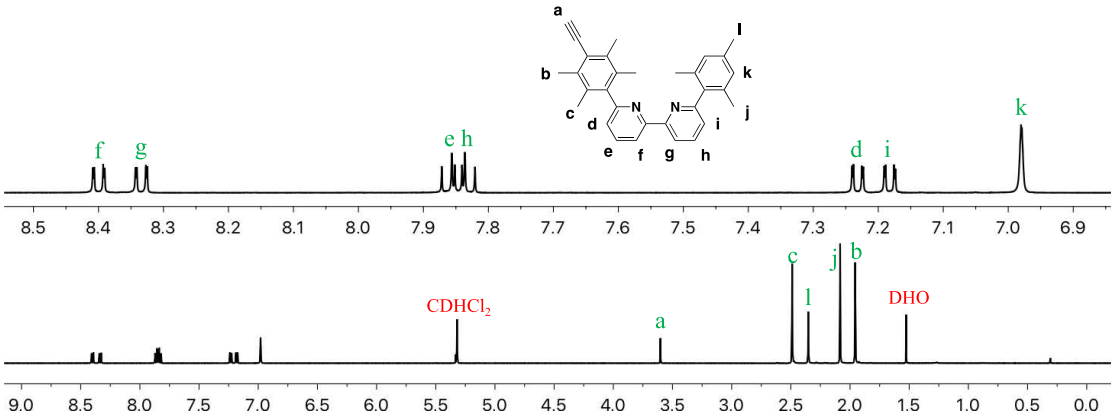

Figure S10. ^{1}H NMR of compound **19** in the CD_2Cl_2 (500 MHz, 298 K)

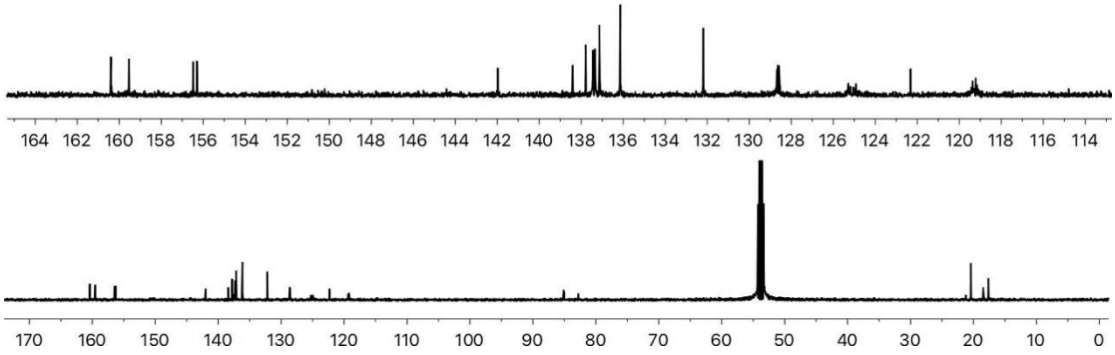

Figure S11. ^{13}C NMR of compound **19** in the CD_2Cl_2 (125 MHz, 298K)

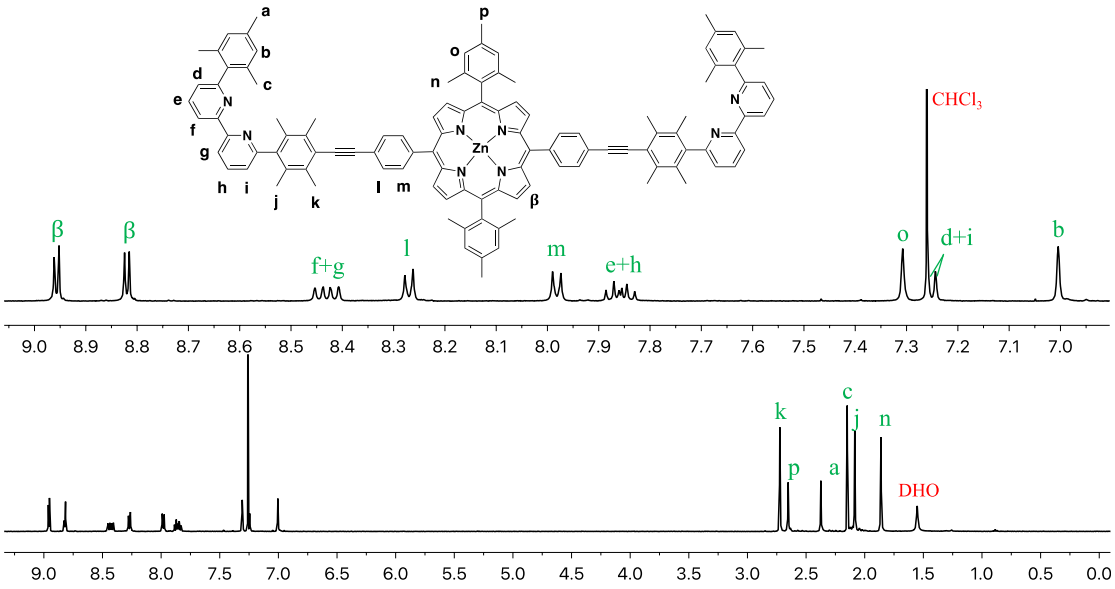

Figure S12. ^{1}H NMR of compound **4** in the $CDCl_3$ (500 MHz, 298 K)

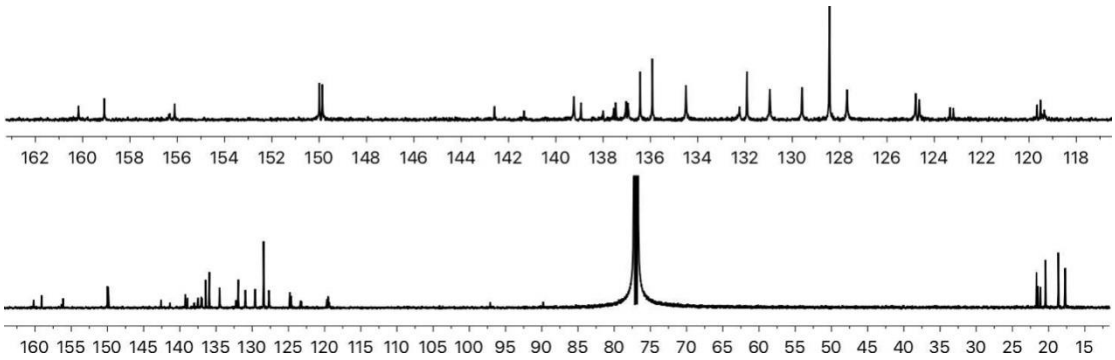

Figure S13. ^{13}C NMR of compound **4** in the $CDCl_3$ (125 MHz, 298 K)

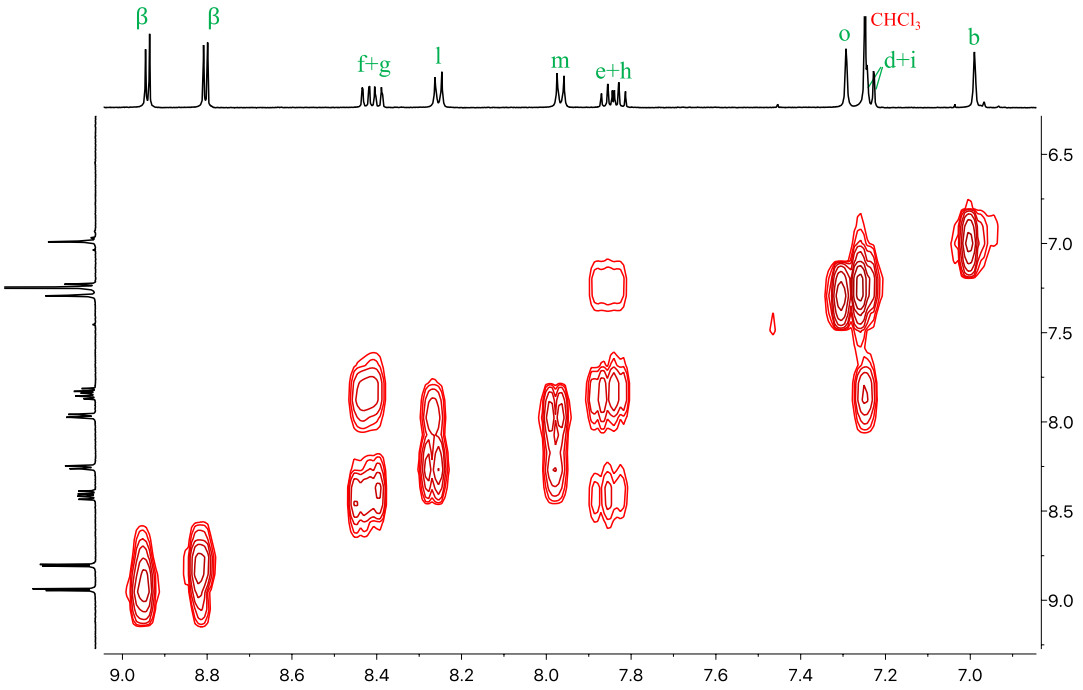

Figure S14. ^{1}H-^{1}H COSY NMR of compound **4** in the $CDCl_3$ (500 MHz, 298 K)

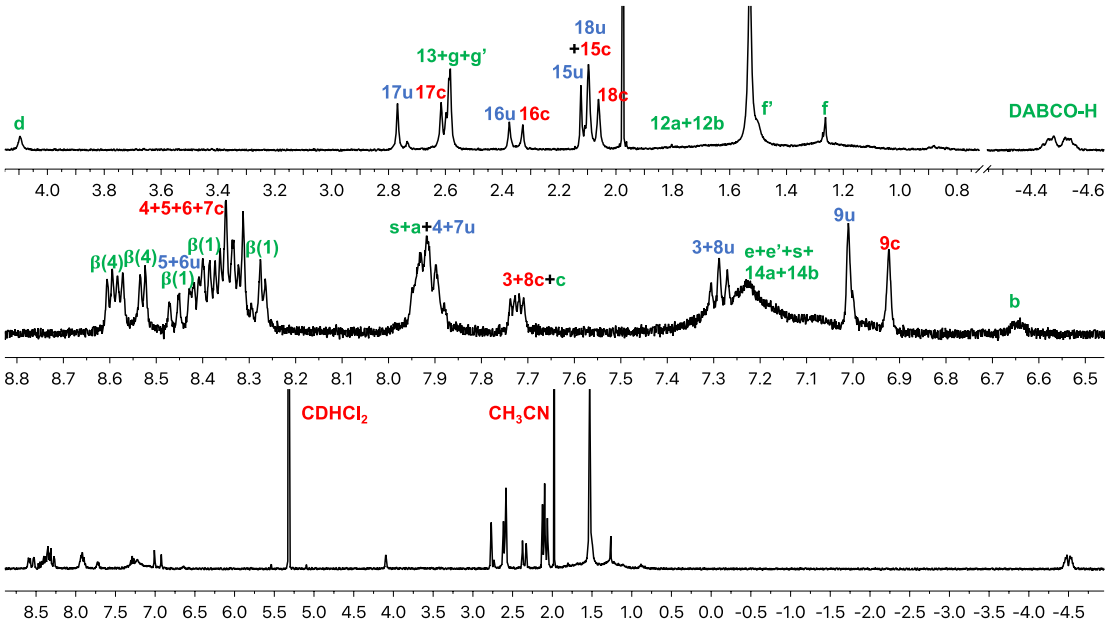

Figure S15. ^{1}H NMR of compound **ROT-1a** in the CD_2Cl_2 (500 MHz, 298 K)

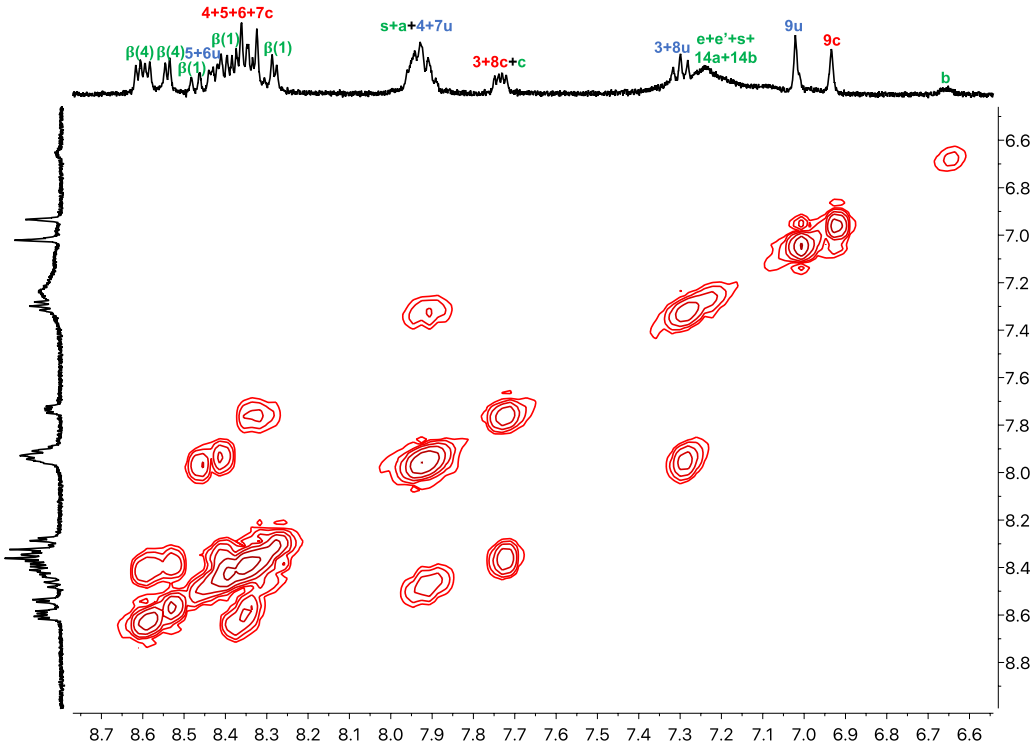

Figure S16. ^{1}H-^{1}H COSY NMR of compound **ROT-1a** in the CD_2Cl_2 (500 MHz, 298 K)

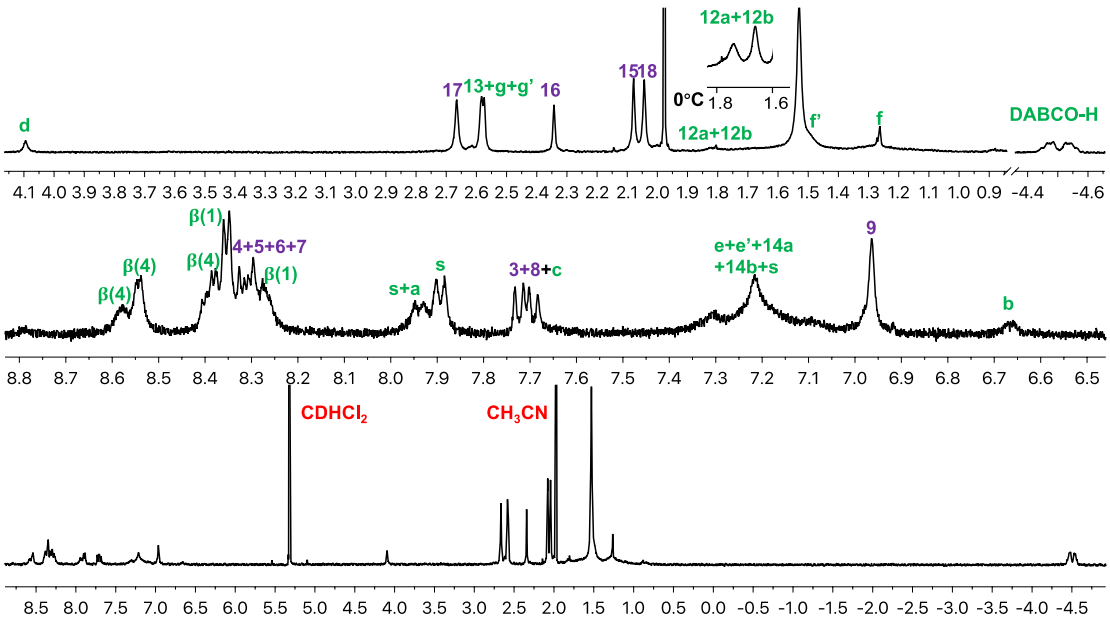

Figure S17. ^{1}H NMR of compound **ROT-1a'** in the CD_2Cl_2 (500 MHz, 298 K)

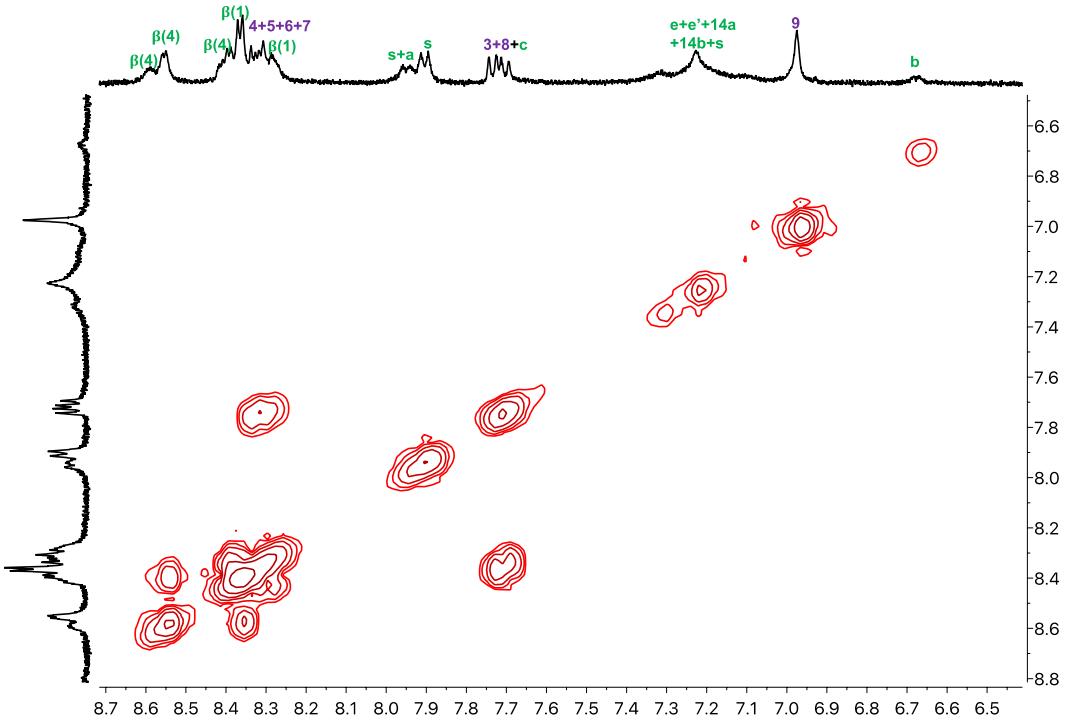

Figure S18. ^{1}H-^{1}H COSY NMR of compound **ROT-1a'** in the CD_2Cl_2 (500 MHz, 298 K)

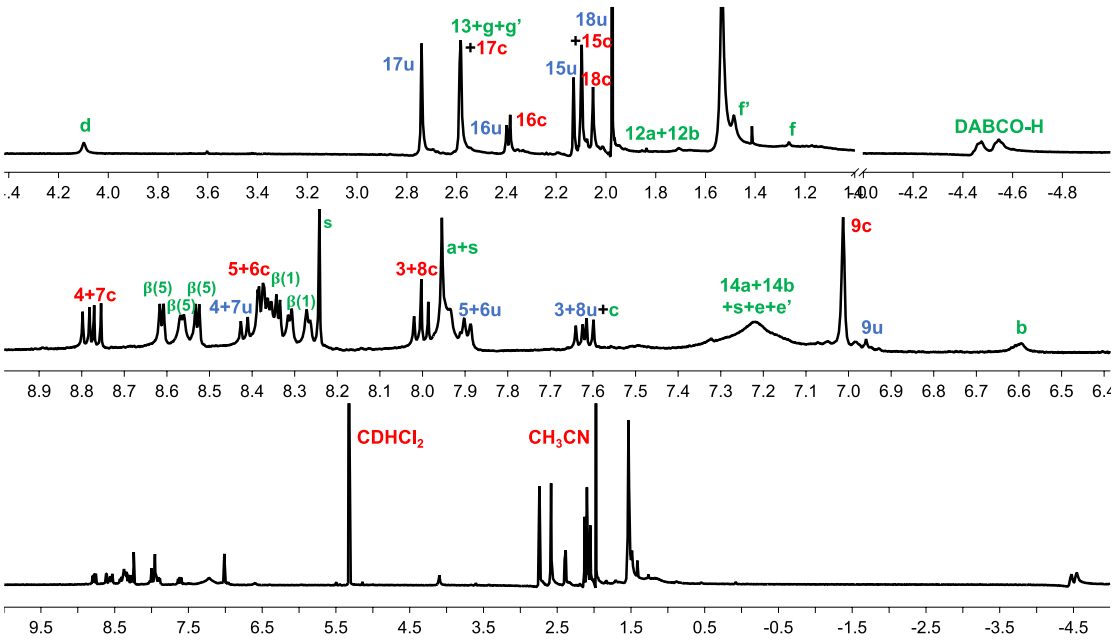

Figure S19. ^{1}H NMR of compound **ROT-1b** in the CD_2Cl_2 (500 MHz, 298 K)

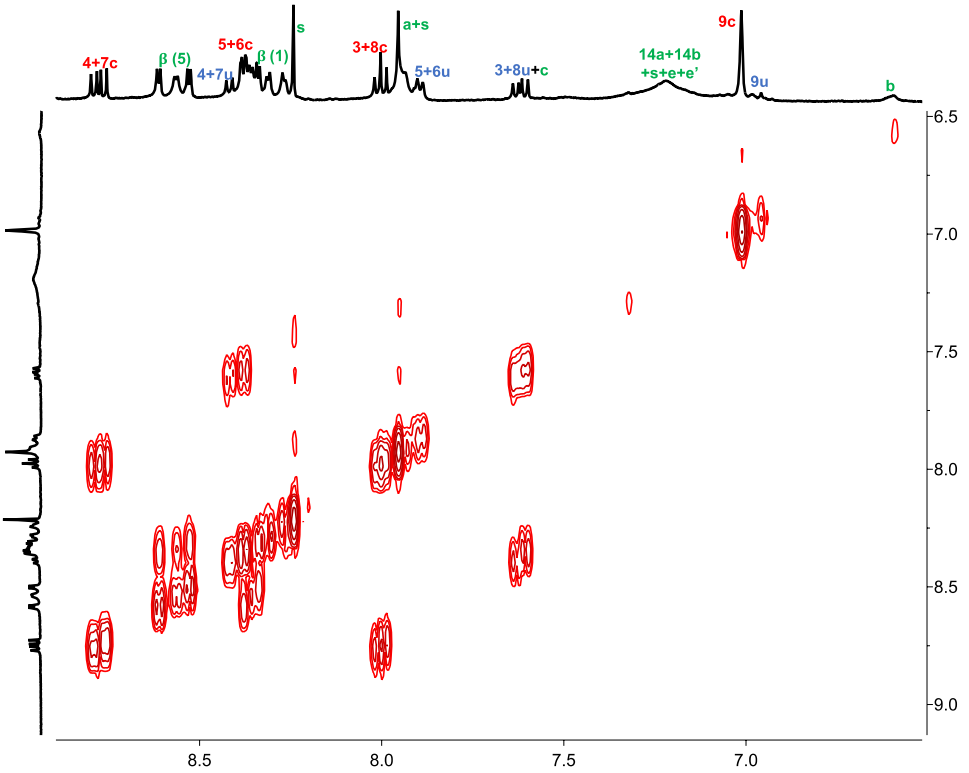

Figure S20. ^{1}H-^{1}H COSY NMR of compound **ROT-1b** in the CD_2Cl_2 (500 MHz, 298 K)

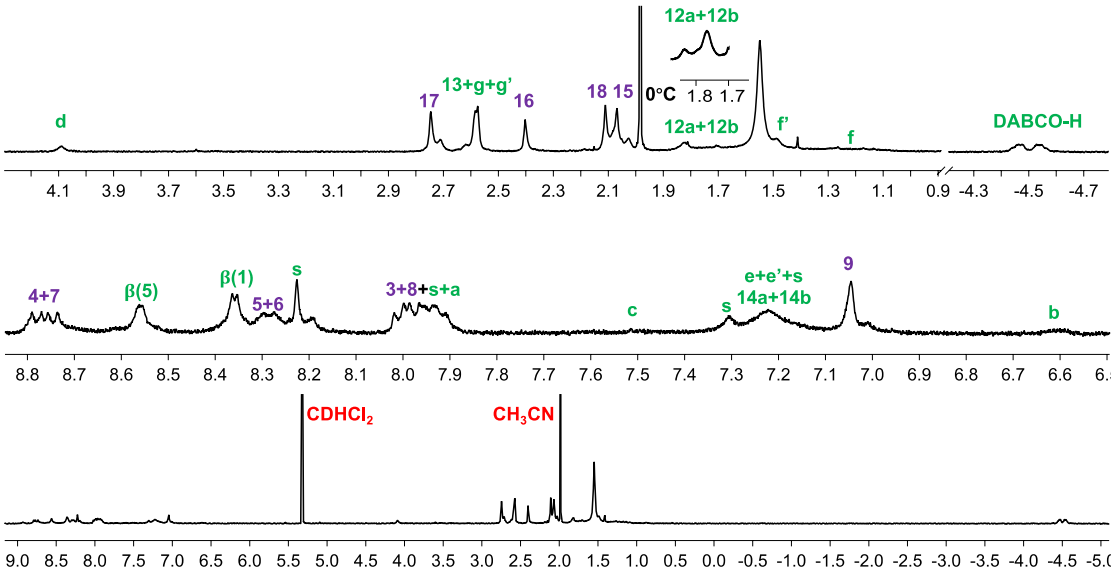

Figure S21. ^{1}H NMR of compound **ROT-1b'** in the CD_2Cl_2 (500 MHz, 298 K)

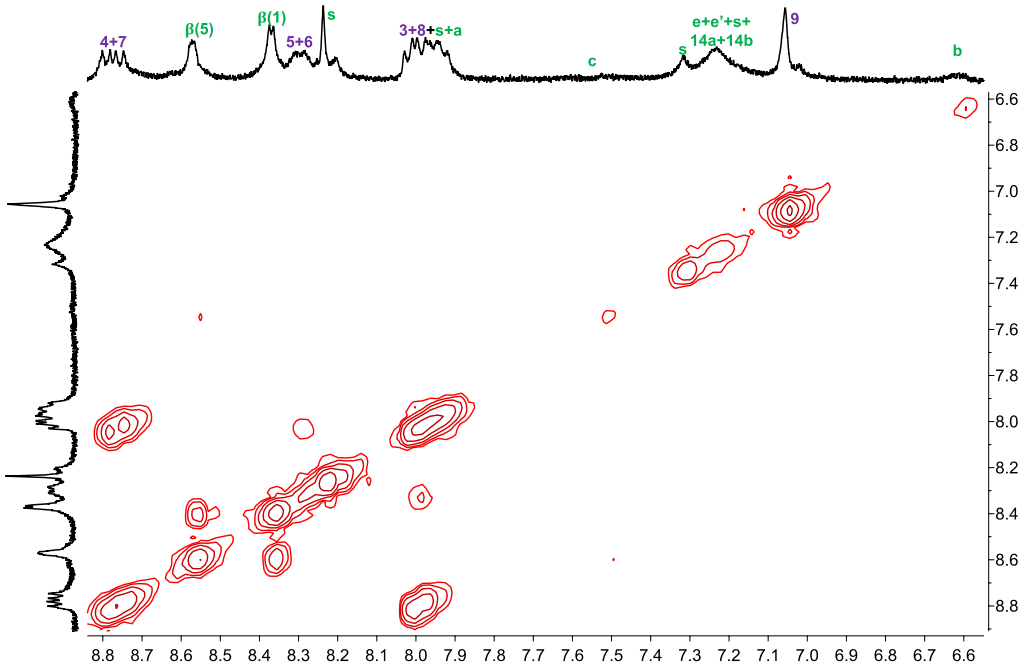

Figure S22. ^{1}H-^{1}H COSY NMR of compound **ROT-1b'** in the CD_2Cl_2 (500 MHz, 298 K)

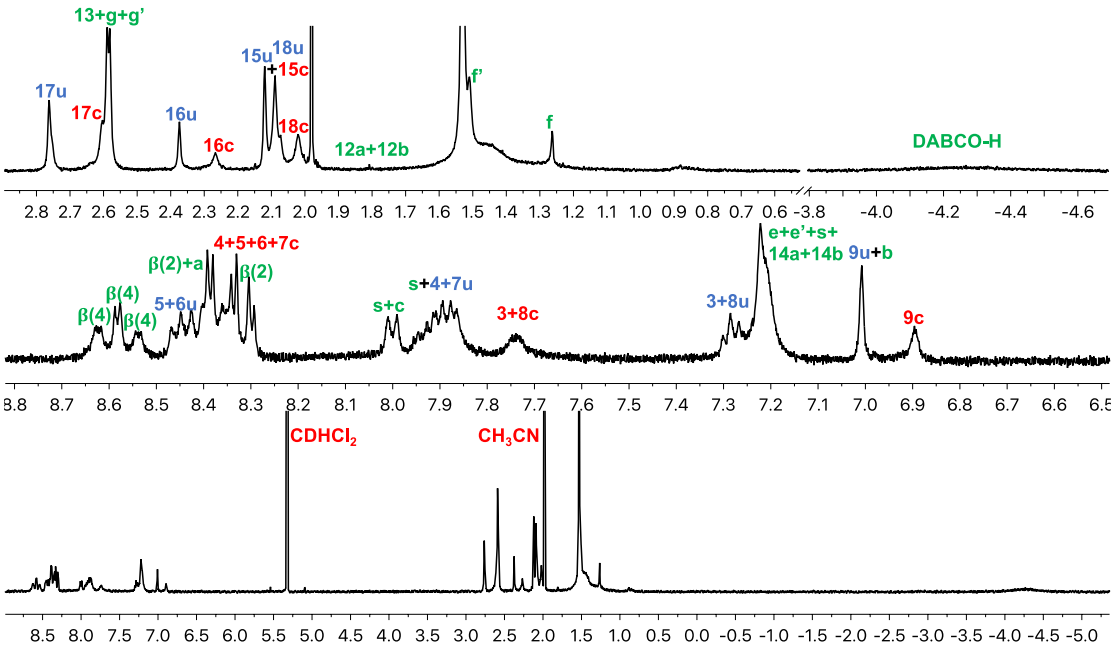

Figure S23. ^{1}H NMR of compound **ROT-2** in the CD_2Cl_2 (500 MHz, 298 K)

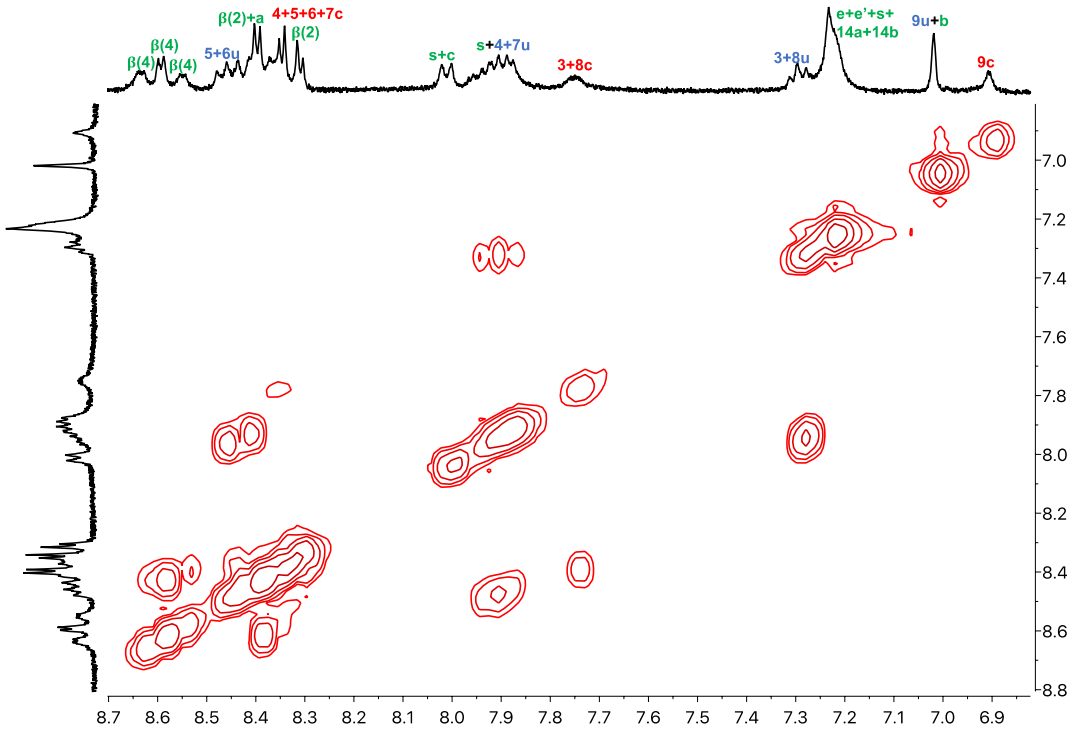

Figure S24. ^{1}H-^{1}H COSY NMR of compound **ROT-2** in the CD_2Cl_2 (500 MHz, 298 K)

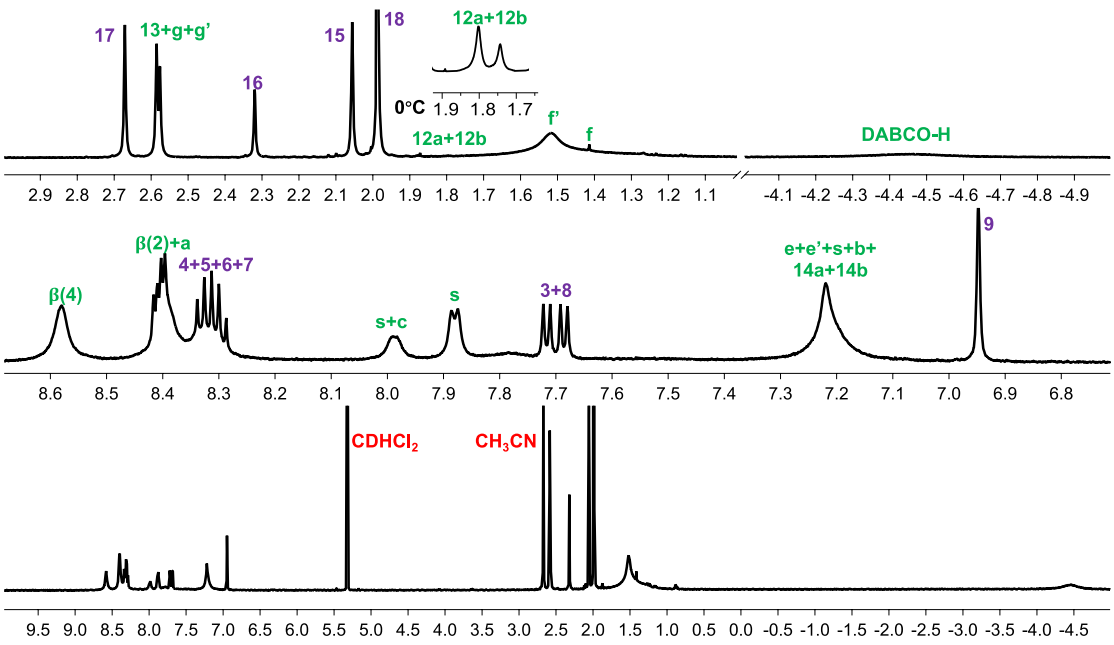

Figure S25. ^{1}H NMR of compound **ROT-2'** in the CD_2Cl_2 (600 MHz, 298 K)

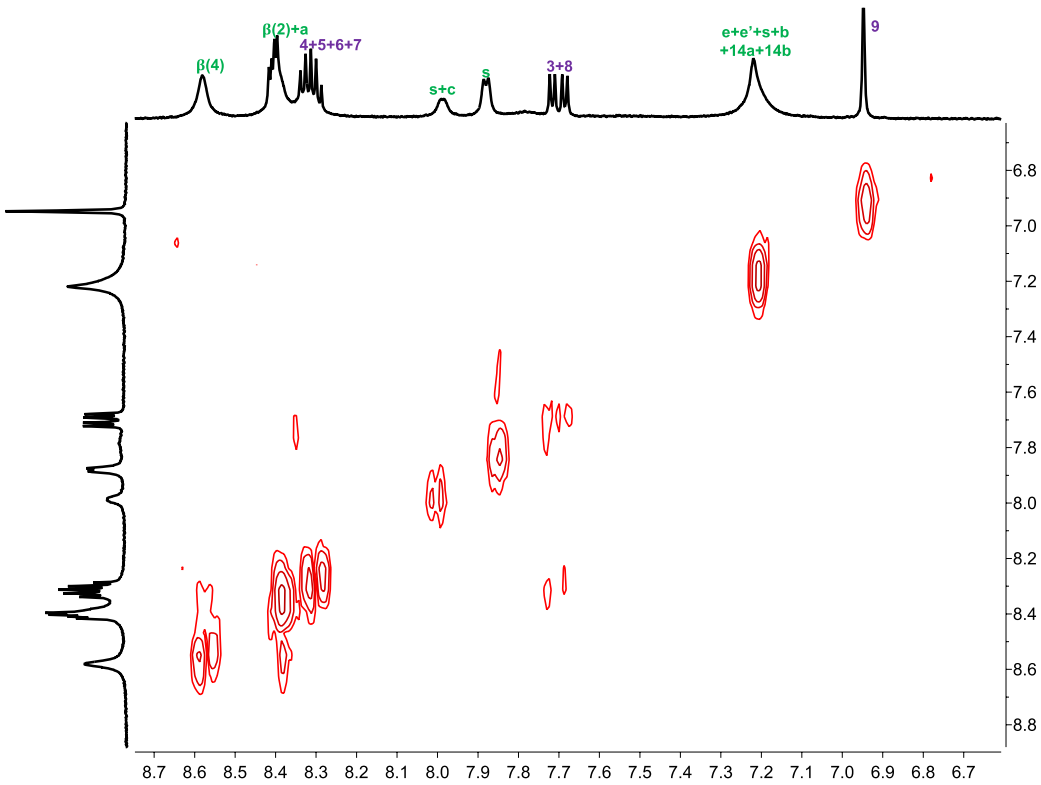

Figure S26. ^{1}H-^{1}H COSY NMR of compound **ROT-2'** in the CD_2Cl_2 (600 MHz, 298 K)

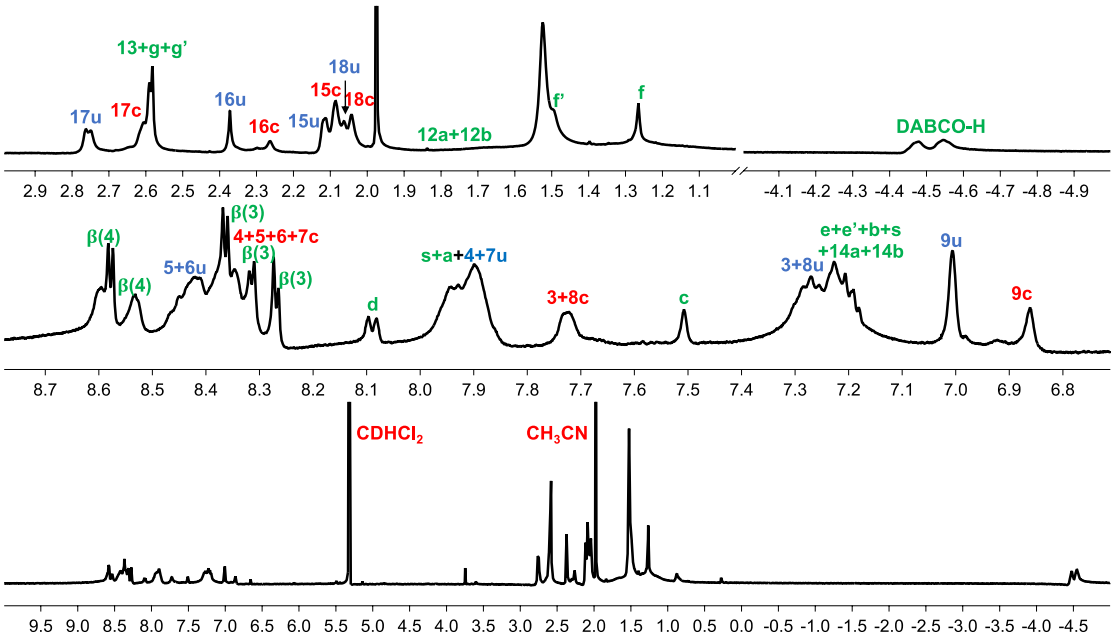

Figure S27. ^{1}H NMR of compound **ROT-3** in the CD_2Cl_2 (500 MHz, 298 K)

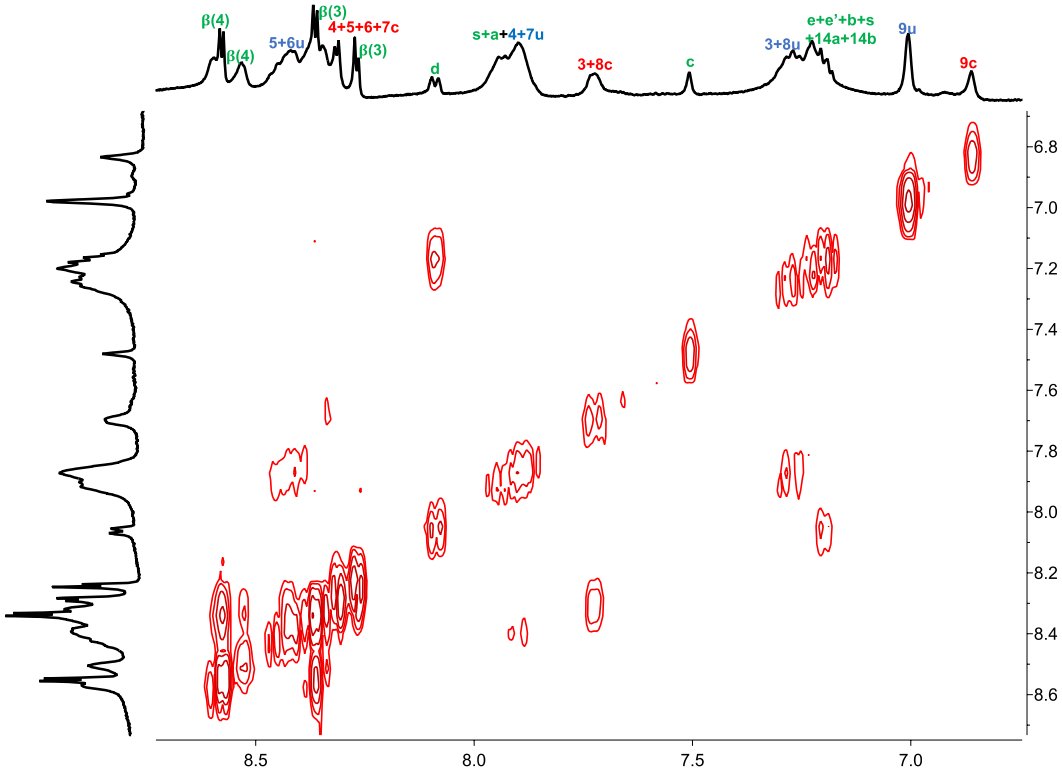

Figure S28. ^{1}H-^{1}H COSY NMR of compound **ROT-3** in the CD_2Cl_2 (500 MHz, 298 K)

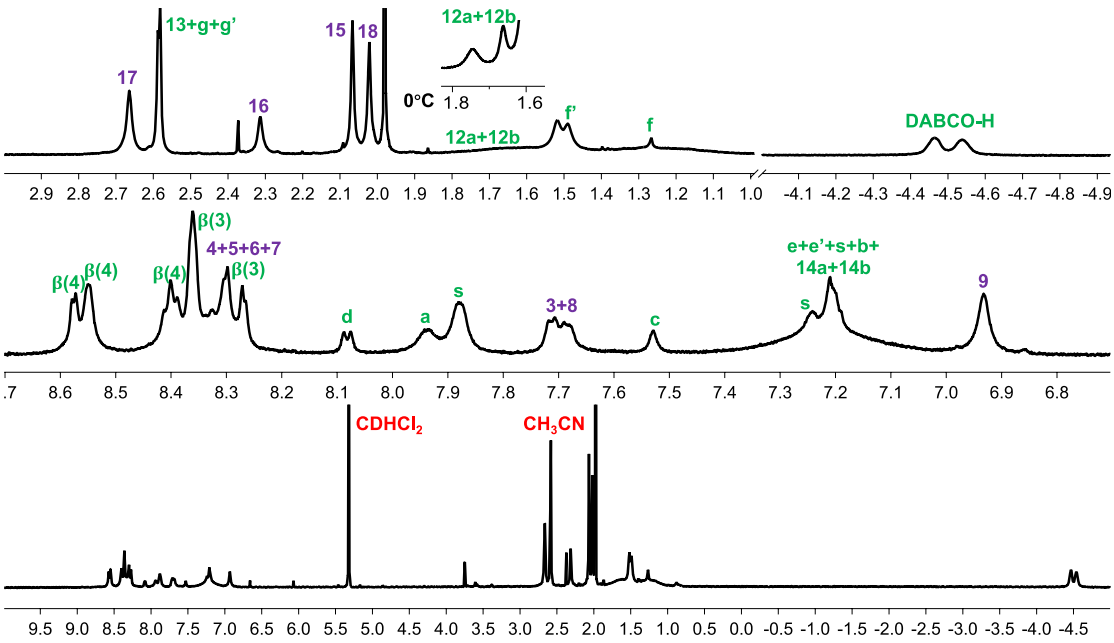

Figure S29. ^{1}H NMR of compound **ROT-3'** in the CD_2Cl_2 (600 MHz, 298 K)

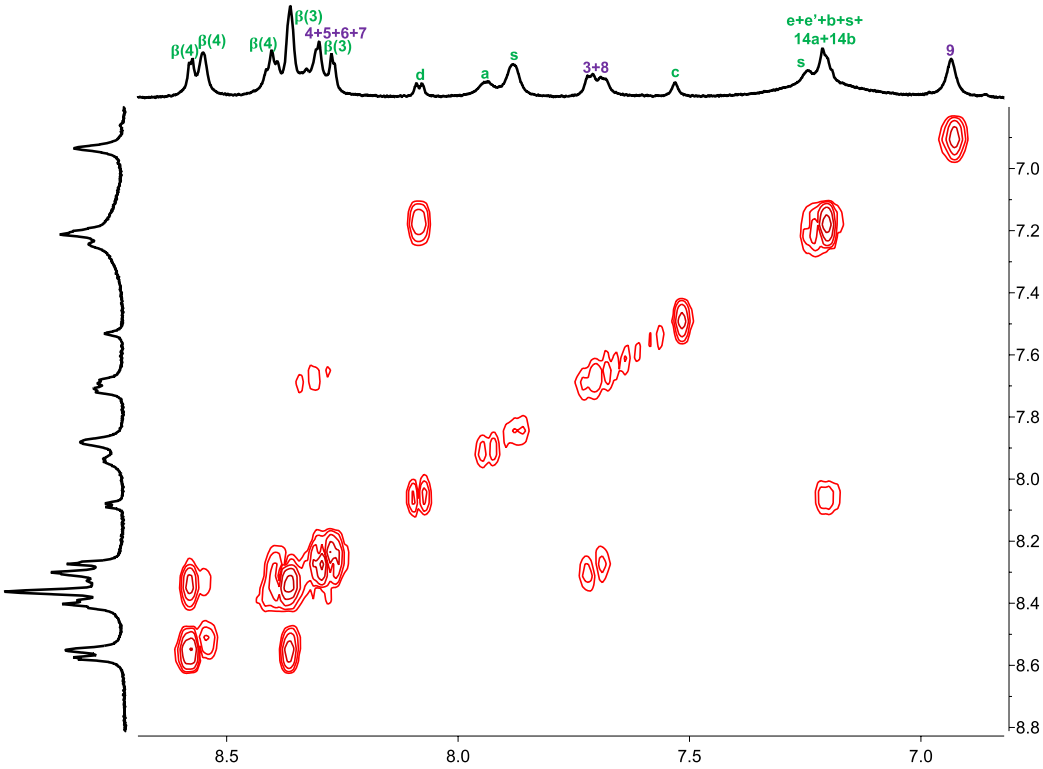

Figure S30. ^{1}H-^{1}H COSY NMR of compound **ROT-3'** in the CD_2Cl_2 (600 MHz, 298K)

3. Variable Temperature ^{1}H NMR Spectra

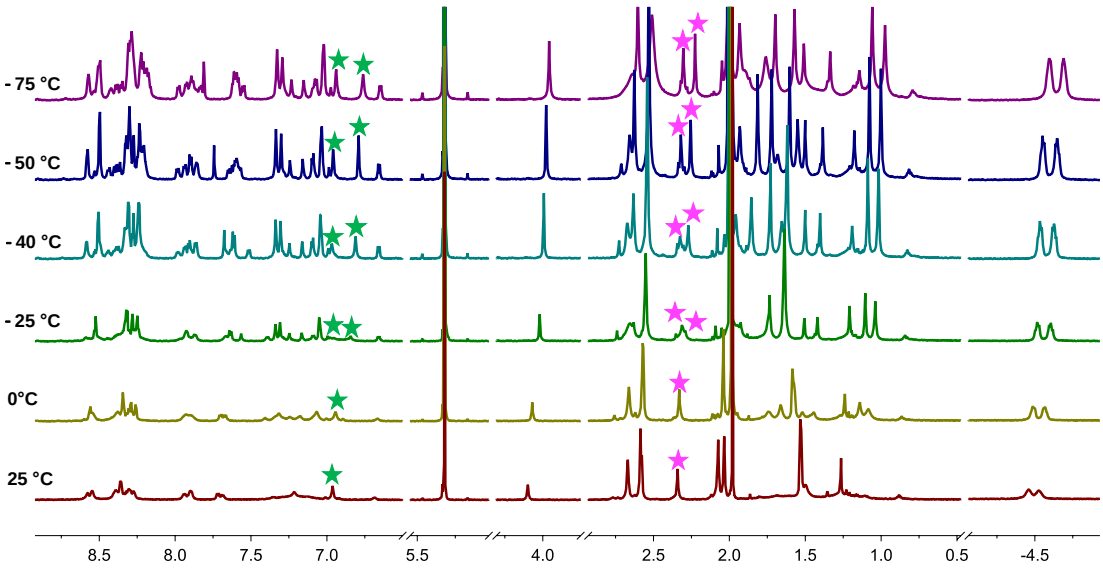

Figure S31. Partial ^{1}H VT-NMR (CD_2Cl_2, 600 MHz) of **ROT-1a'** showing the splitting of proton 9-H (green asterisk marked) and 16-H (magenta asterisk marked).

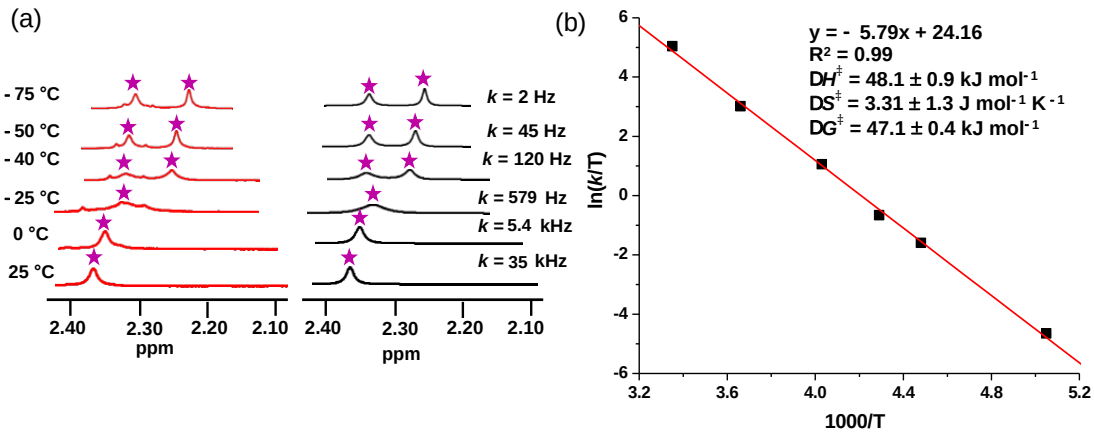

Figure S32. Simulated and experimental ^{1}H VT-NMR (CD_2Cl_2, 600 MHz) of **ROT-1a'** show the splitting of 16-H (red magenta asterisk marked) and (b) Eyring plot for rotational exchange in **ROT-1a'**.

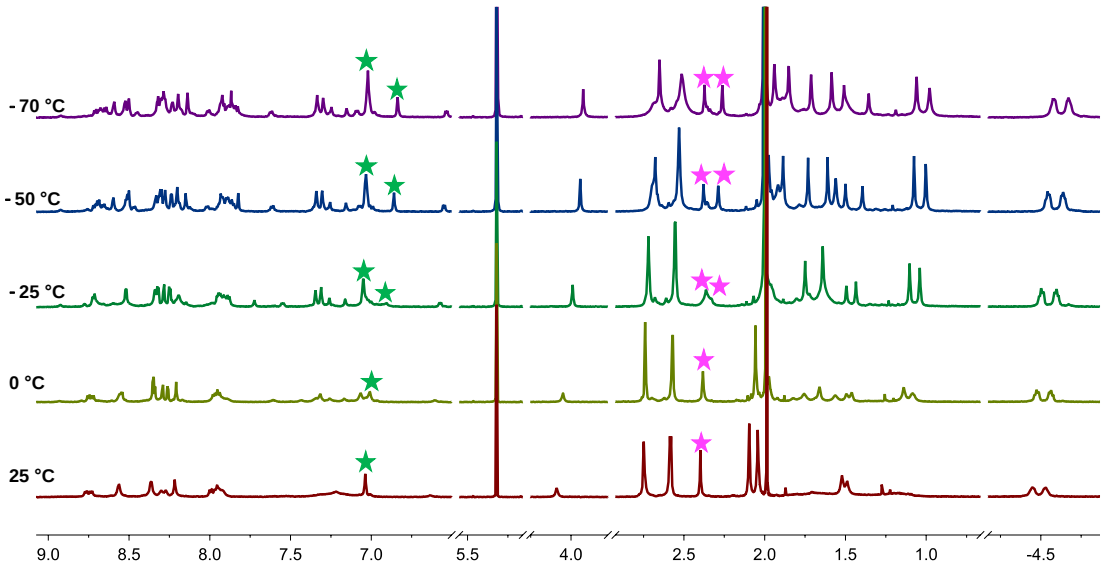

Figure S33. Partial ^{1}H VT-NMR (CD_2Cl_2, 600 MHz) of **ROT-1b'** showing the splitting of proton 9-H (green asterisk marked) and 16-H (magenta asterisk marked).

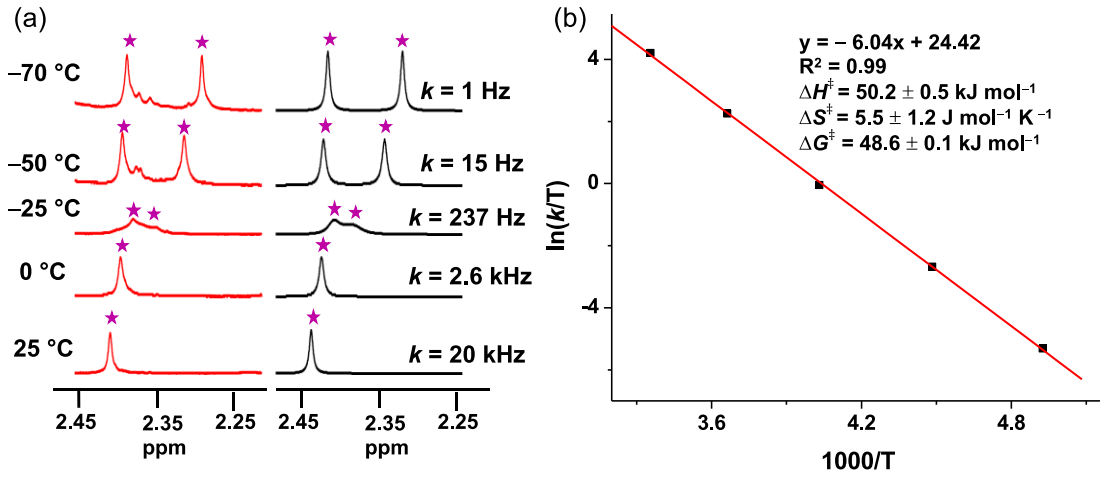

Figure S34. Simulated and experimental ^{1}H VT-NMR (CD_2Cl_2, 600 MHz) of **ROT-1b'** show the splitting of 16-H (red magenta asterisk marked) and (b) Eyring plot for rotational exchange in **ROT-1b'**.

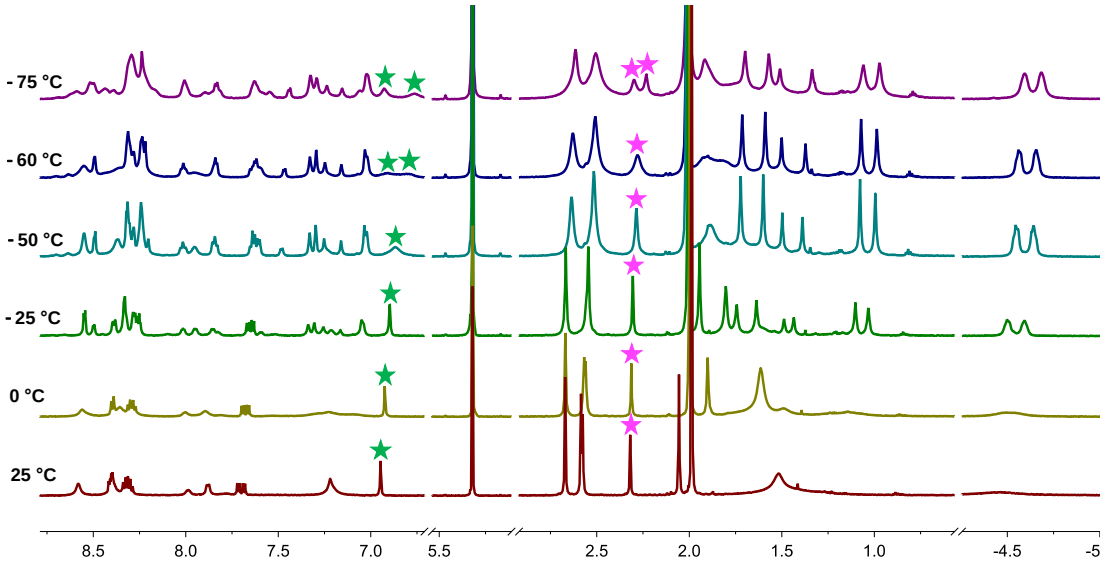

Figure S35. Partial ^{1}H VT-NMR (CD_2Cl_2, 600 MHz) of **ROT-2'** showing the splitting of proton 9-H (green asterisk marked) and 16-H (magenta asterisk marked).

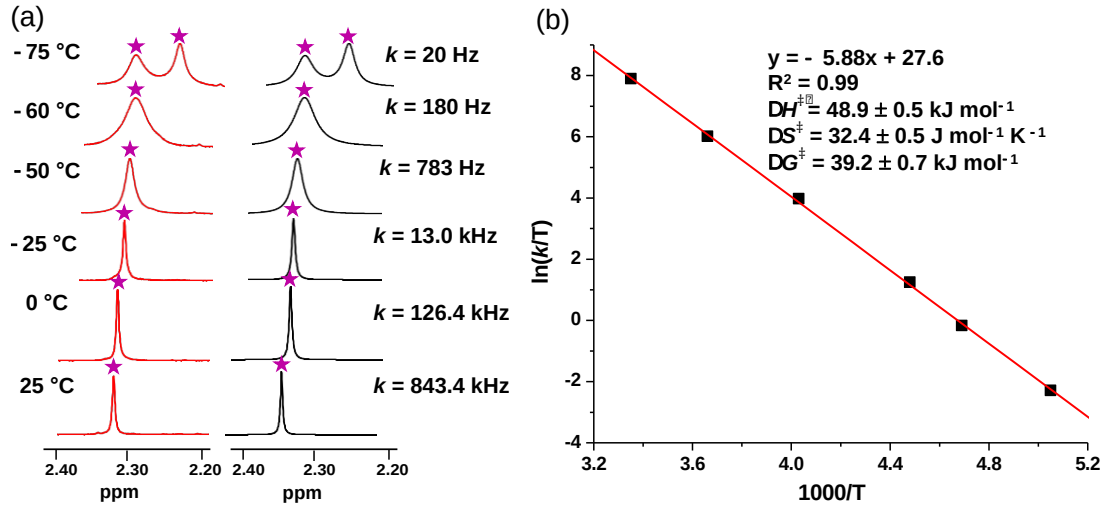

Figure S36. Simulated and experimental ^{1}H VT-NMR (CD_2Cl_2, 600 MHz) of **ROT-2'** show the splitting of 16-H (red magenta asterisk marked) and (b) Eyring plot for rotational exchange in **ROT-2'**.

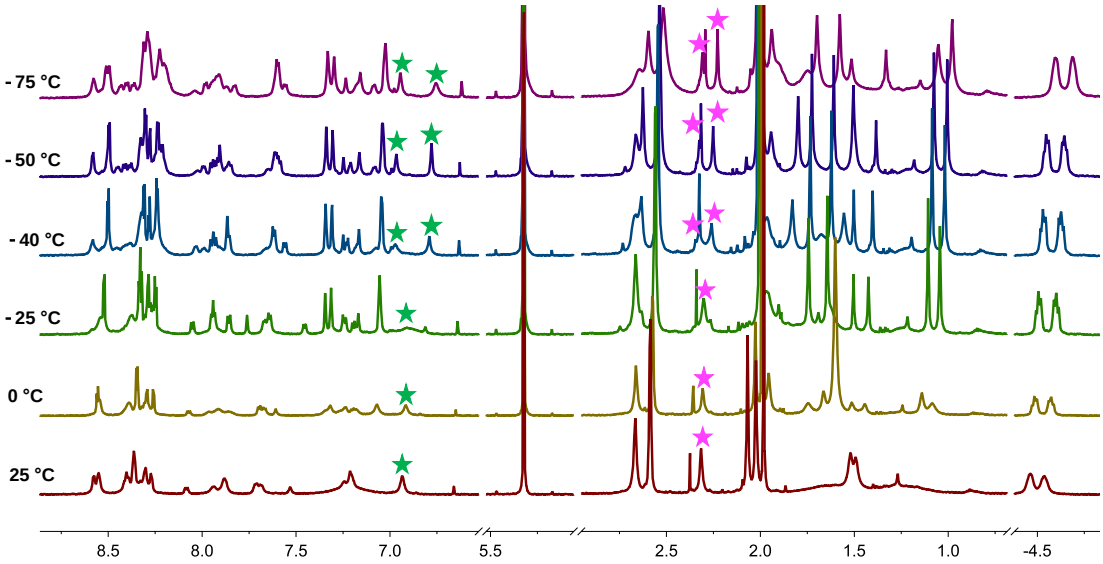

Figure S37. Partial ^{1}H VT-NMR (CD_2Cl_2, 600 MHz) of **ROT-3'** showing the splitting of proton 9-H (green asterisk marked) and 16-H (magenta asterisk marked).

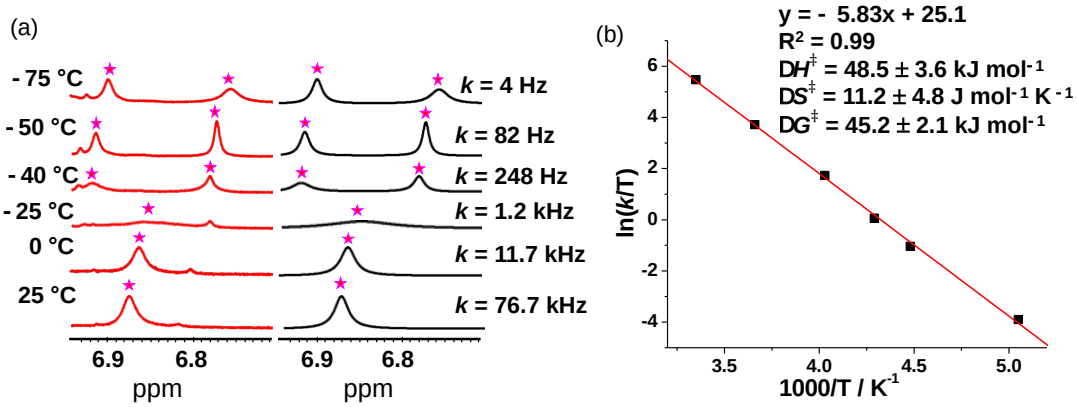

Figure S38. Simulated and experimental ^{1}H VT-NMR (CD_2Cl_2, 600 MHz) of **ROT-3'** shows the splitting of 9-H (red magenta asterisk marked) and (b) Eyring plot for rotational exchange in **ROT-3'**.

4. DOSY NMR Spectra

Calculation of hydrodynamic radius from DOSY

The diffusion coefficient *D* (of **ROT-1a'**, **ROT-1b'**, **ROT-2'** and **ROT-3'**) was obtained from the DOSY spectrum and corresponding hydrodynamic radius was calculated by using the Stokes-Einstein equation:

$$r = k_B T / 6\pi\eta D$$

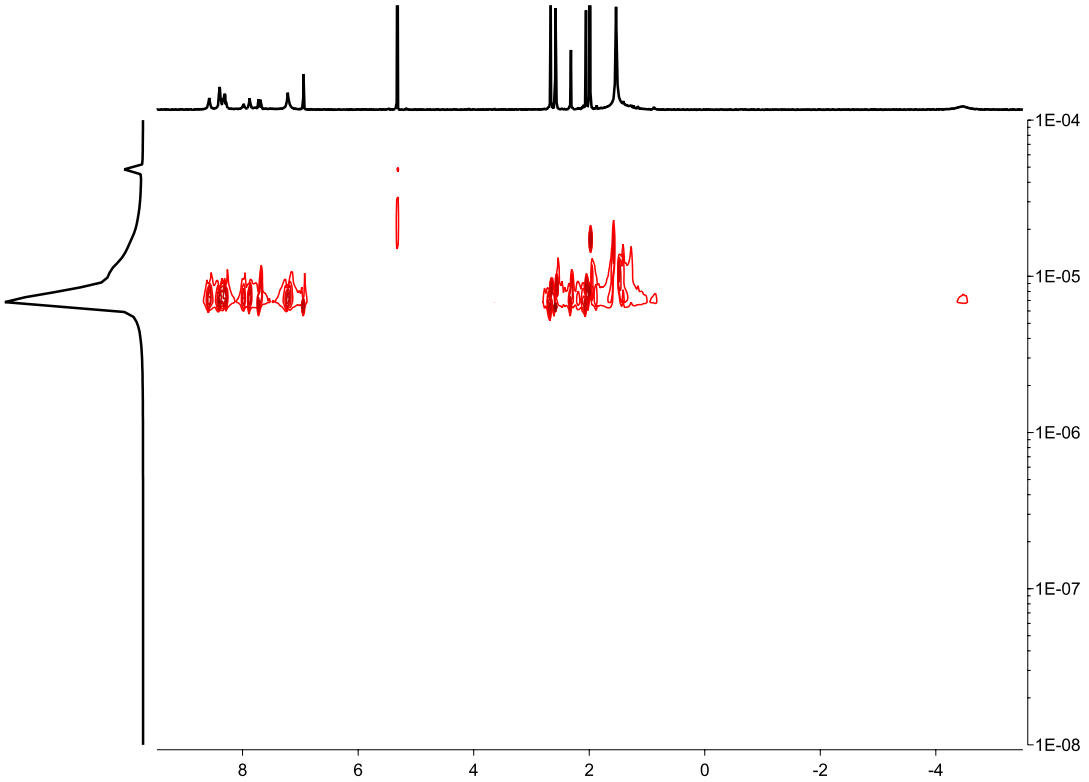

Figure S39. ^{1}H-DOSY NMR of **ROT-1a'** in CD_2Cl_2 (600 MHz, 298 K) Diffusion coefficient D = 5.0 × 10^{-10} m^2 s^{-1}, hydrodynamic radius r = 10.6 Å.

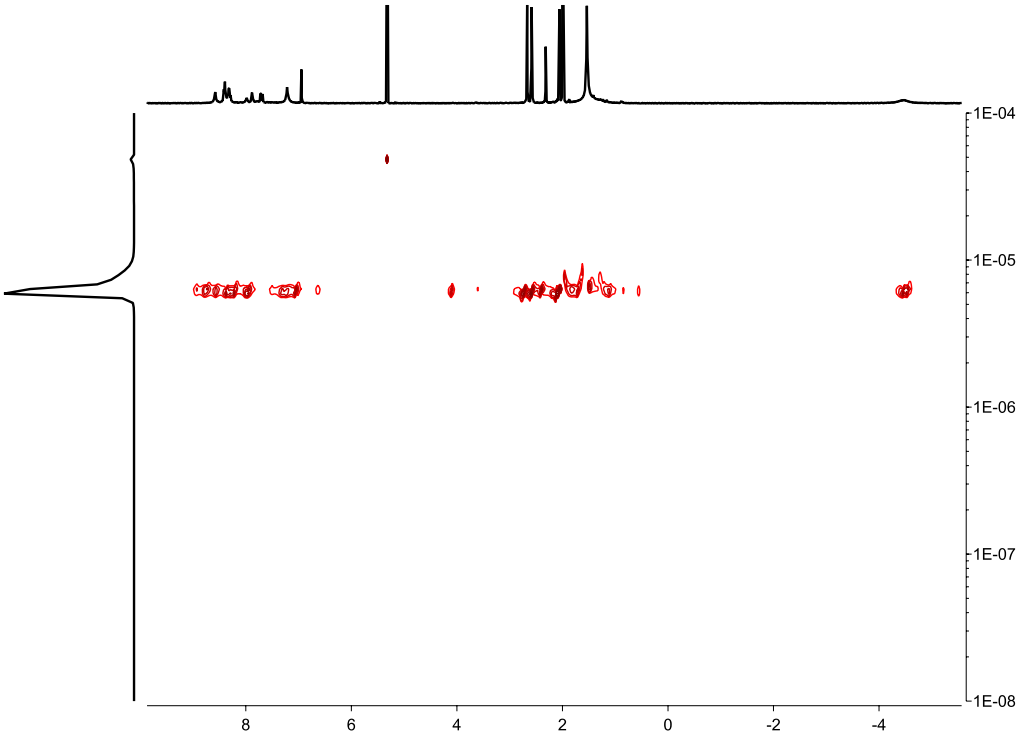

Figure S40. ^{1}H-DOSY NMR of **ROT-1b'** in CD_2Cl_2 (600 MHz, 298 K) Diffusion coefficient D = 4.4 × 10^{-10} m^2 s^{-1}, hydrodynamic radius r = 12.0 Å.

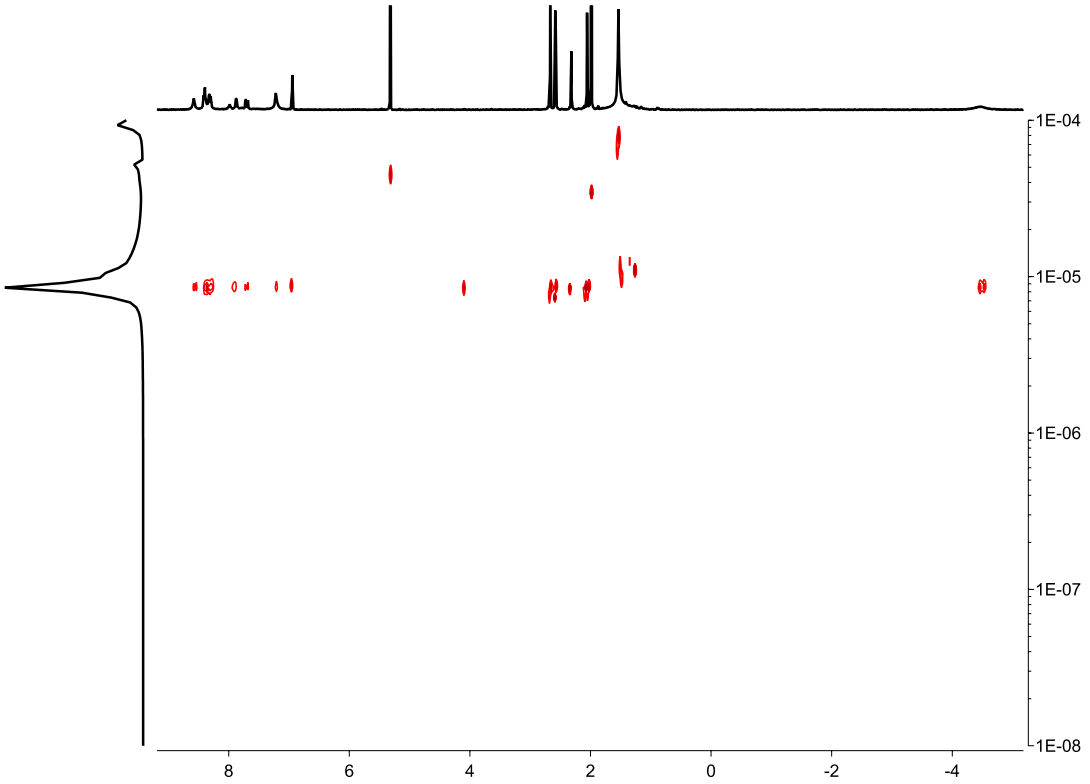

Figure S41. ^{1}H-DOSY NMR of **ROT-2'** in CD_2Cl_2 (600 MHz, 298 K) Diffusion coefficient D = 6.0 × 10^{-10} m^2 s^{-1}, hydrodynamic radius r = 8.8 Å.

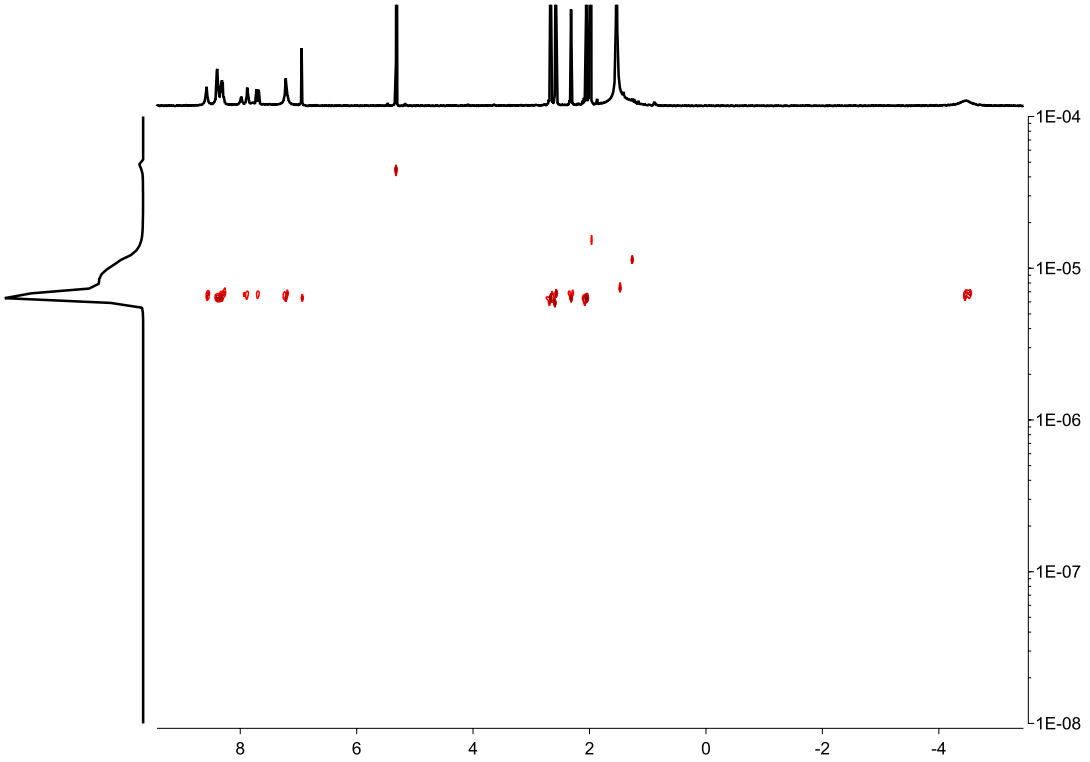

Figure S42. ^{1}H-DOSY NMR of **ROT-3'** in CD_2Cl_2 (600 MHz, 298 K) Diffusion coefficient D = 4.6 × 10^{-10} m^2 s^{-1}, hydrodynamic radius r = 11.5 Å.

5. ESI-MS Spectra

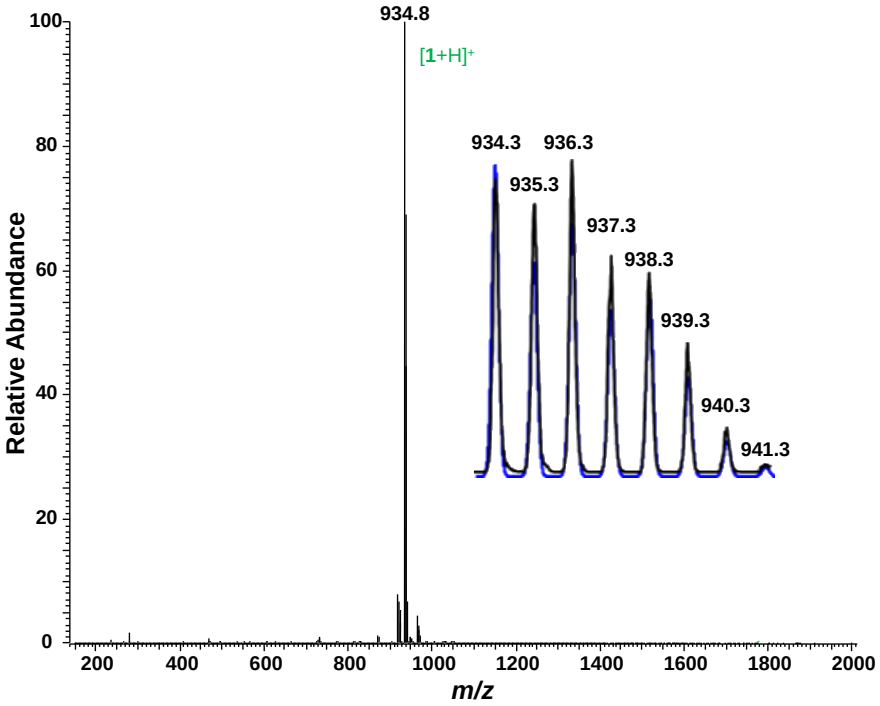

Figure S43. ESI-MS spectrum of compound **1** in CH_2Cl_2. The blue trace represents the theoretical isotopic splitting of the compound [**1**+H]$^+$.

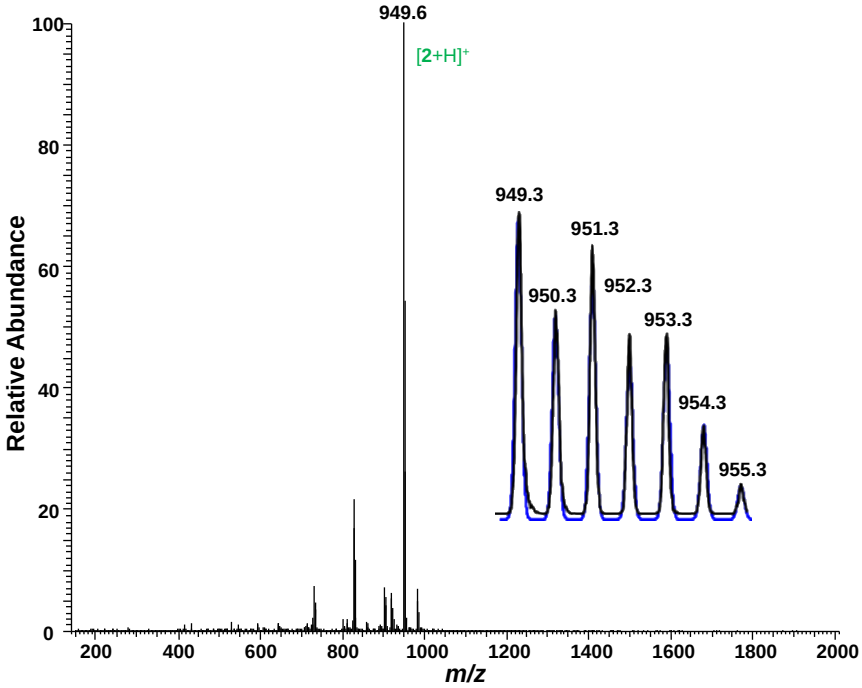

Figure S44. ESI-MS spectrum of compound **2** in CH_2Cl_2. The blue trace represents the theoretical isotopic splitting of the compound [**2**+H]$^+$.

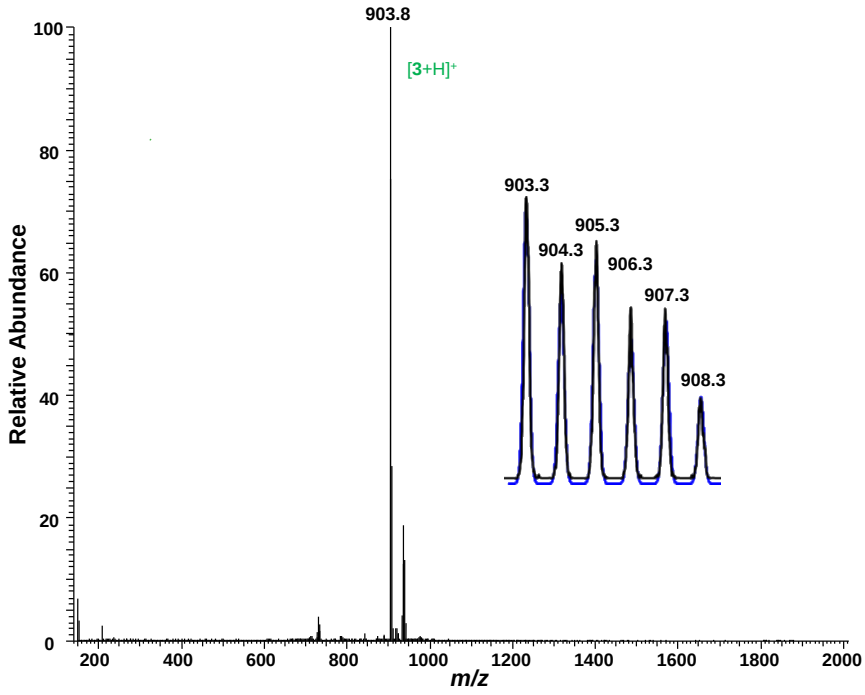

Figure S45. ESI-MS spectrum of compound **3** in CH_2Cl_2. The blue trace represents the theoretical isotopic splitting of the compound [**3**+H]$^+$.

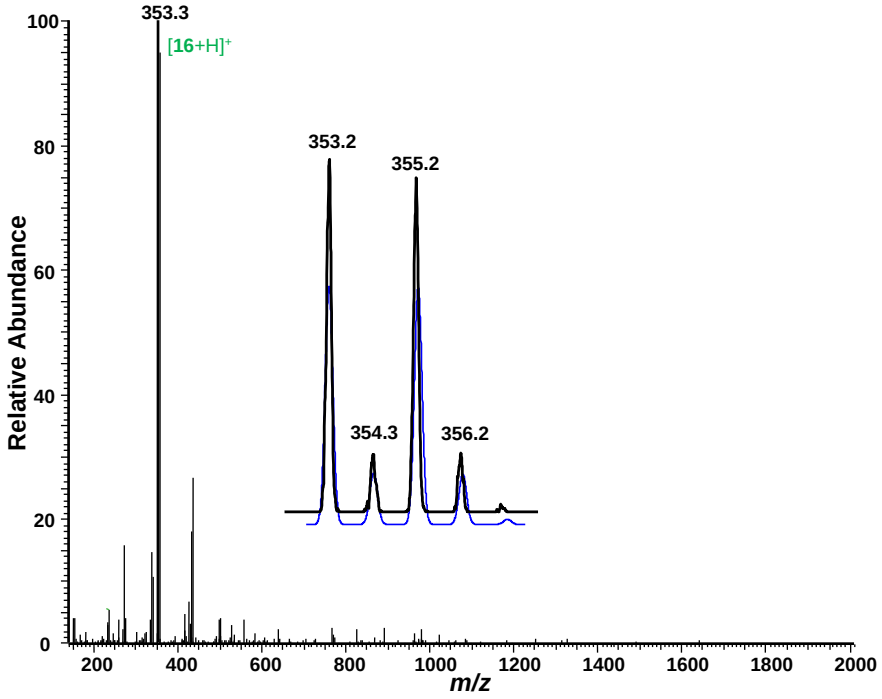

Figure S46. ESI-MS spectrum of compound **16** in CH_2Cl_2. The blue trace represents the theoretical isotopic splitting of the compound [**16**+H]$^+$.

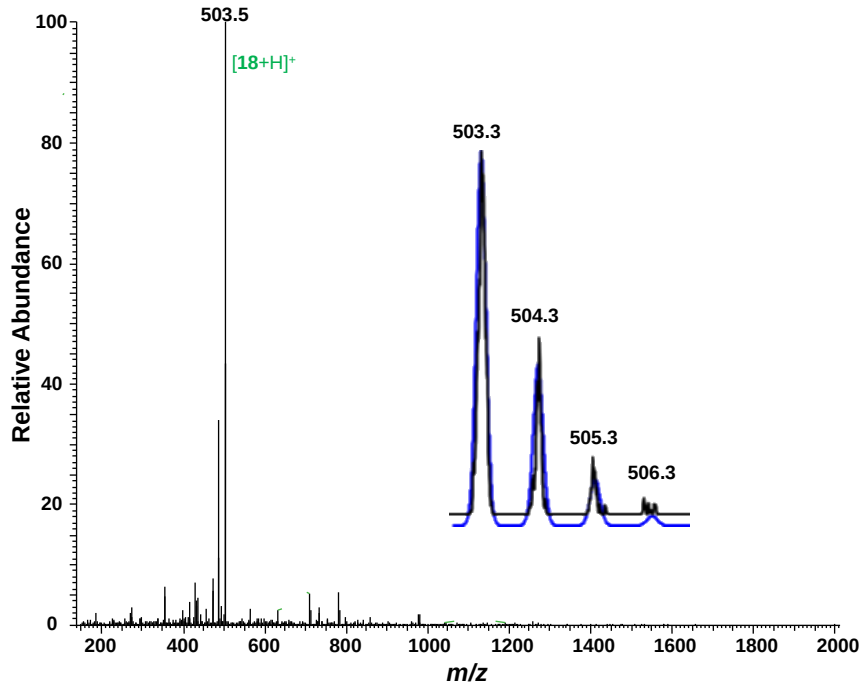

Figure S47. ESI-MS spectrum of compound **18** in CH_2Cl_2. The blue trace represents the theoretical isotopic splitting of the compound [**18**+H]$^+$.

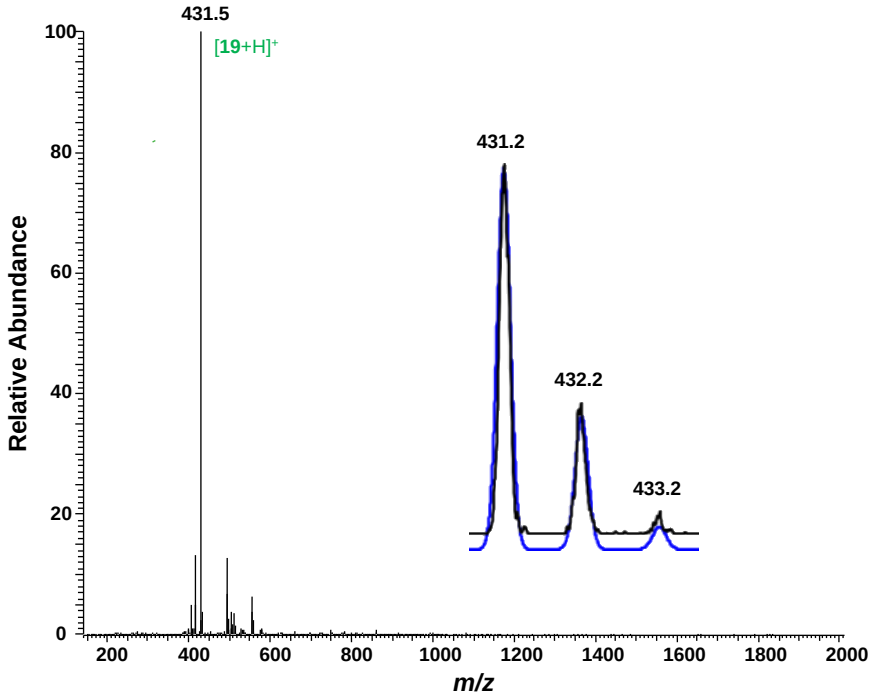

Figure S48. ESI-MS spectrum of compound **19** in CH_2Cl_2**.** The blue trace represents the theoretical isotopic splitting of the compound [**19**+H]$^+$.

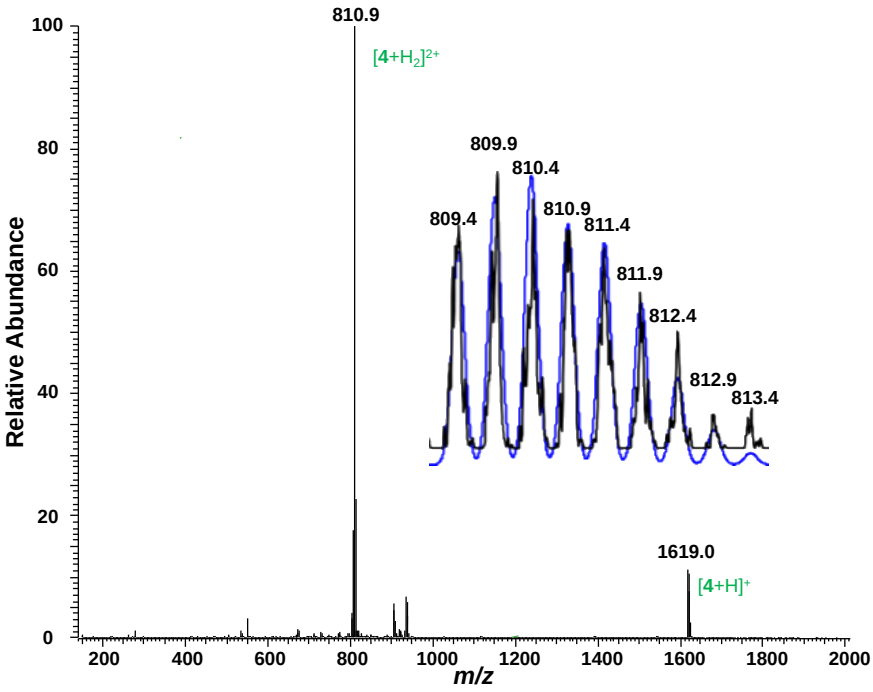

Figure S49. ESI-MS spectrum of compound **4** in CH_2Cl_2. The blue trace represents the theoretical isotopic splitting of the protonated compound $[\mathbf{4}+H_2]^{2+}$.

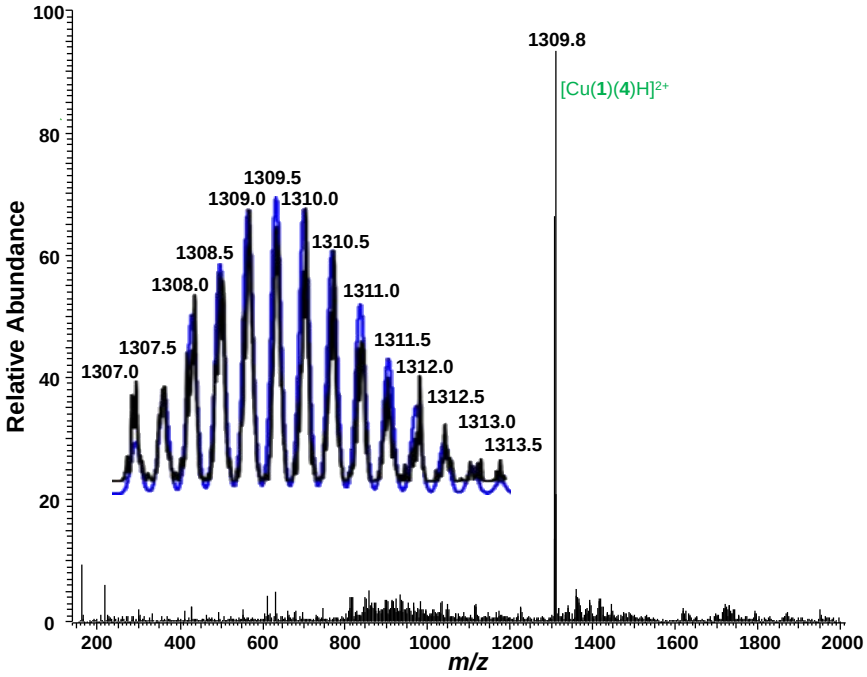

Figure S50. ESI-MS spectrum of compound **ROT-1a** in CH_2Cl_2. The blue trace represents the theoretical isotopic splitting of the complex $[Cu(\mathbf{1})(\mathbf{4})H]^{2+}$.

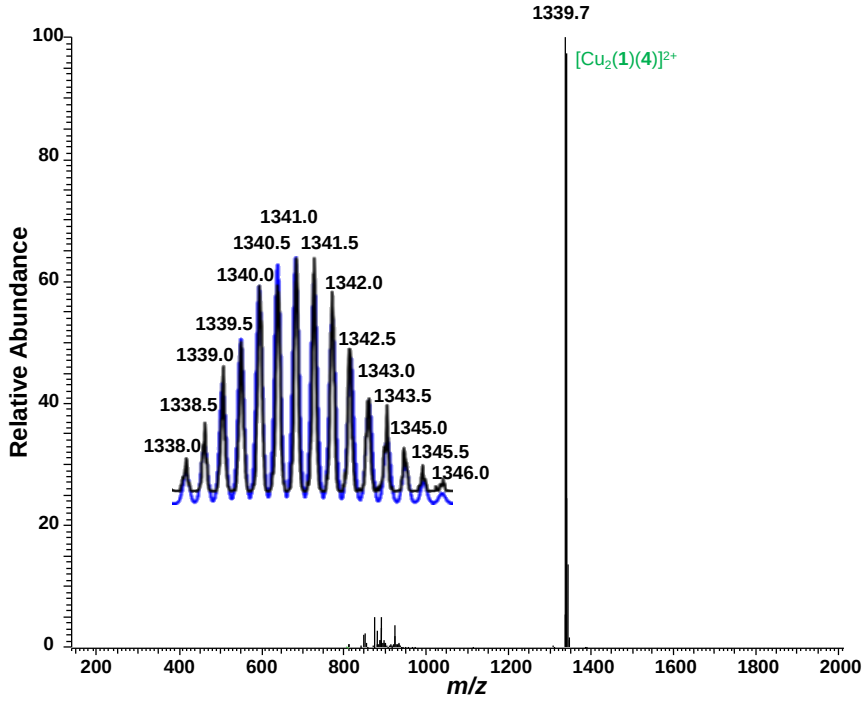

Figure S51. ESI-MS spectrum of compound **ROT-1a'** in CH_2Cl_2. The blue trace represents the theoretical isotopic splitting of the complex $[Cu_2(\mathbf{1})(\mathbf{4})]^{2+}$.

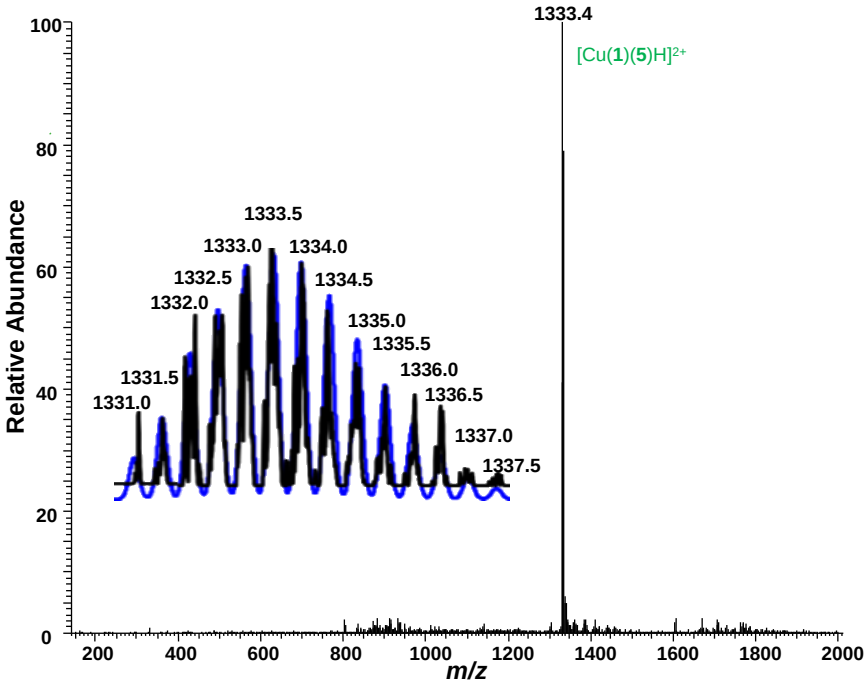

Figure S52. ESI-MS spectrum of compound **ROT-1b** in CH_2Cl_2. The blue trace represents the theoretical isotopic splitting of the complex $[Cu(\mathbf{1})(\mathbf{5})H]^{2+}$.

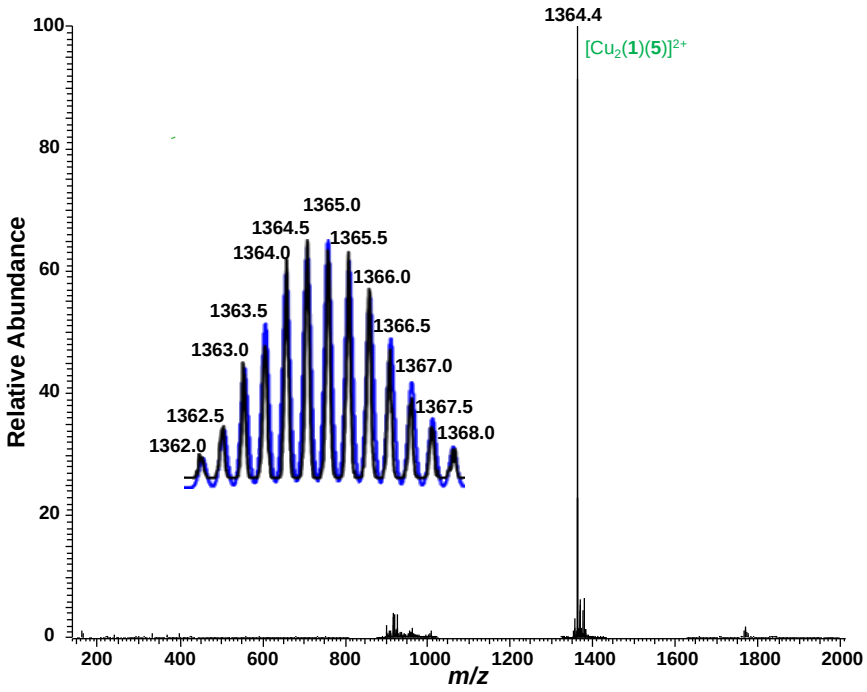

Figure S53. ESI-MS spectrum of compound **ROT-1b'** in CH_2Cl_2. The blue trace represents the theoretical isotopic splitting of the complex $[Cu_2(\mathbf{1})(\mathbf{5})]^{2+}$.

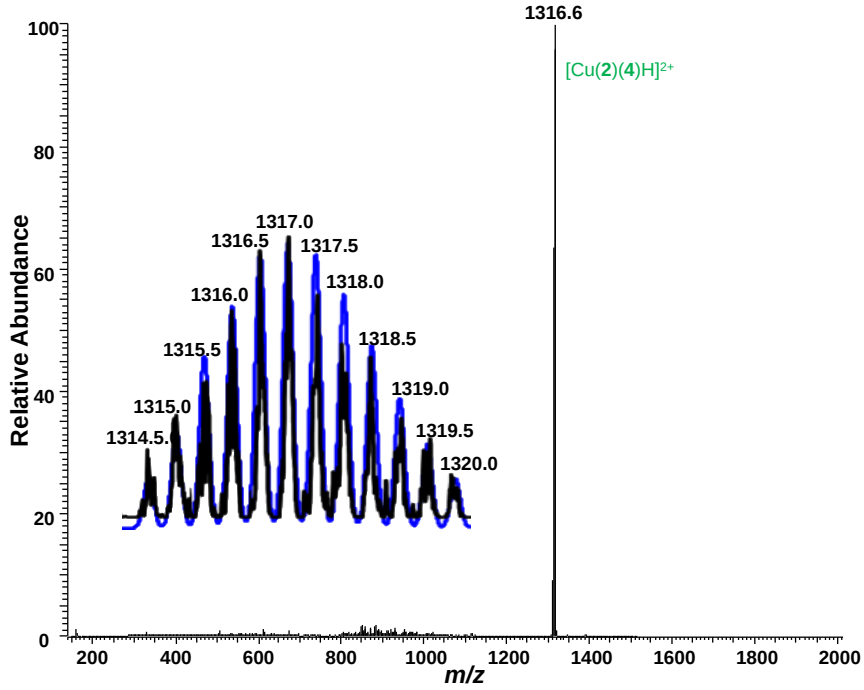

Figure S54. ESI-MS spectrum of compound **ROT-2** in CH_2Cl_2. The blue trace represents the theoretical isotopic splitting of the complex $[Cu(\mathbf{2})(\mathbf{4})H]^{2+}$.

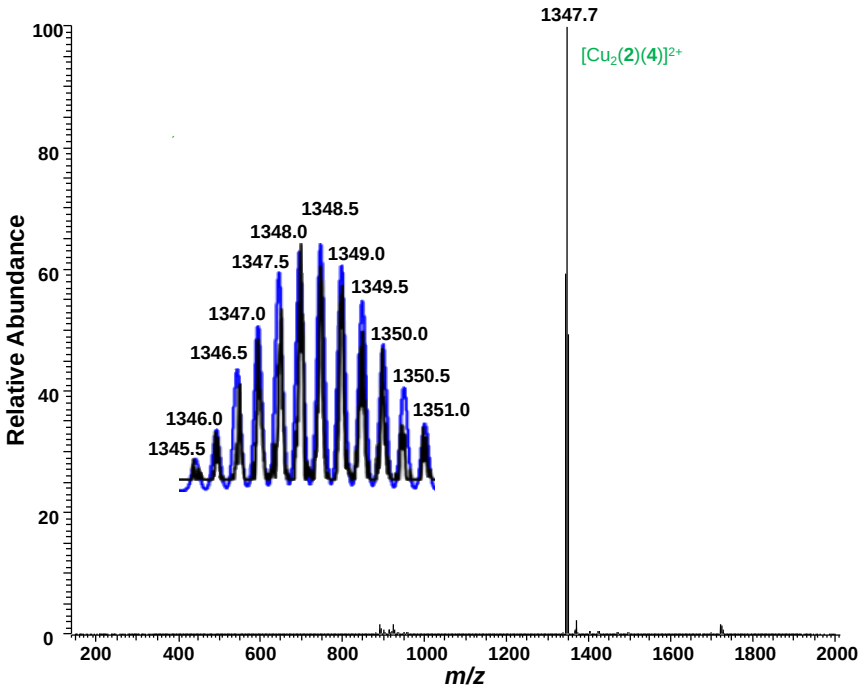

Figure S55. ESI-MS spectrum of compound **ROT-2'** in CH_2Cl_2. The blue trace represents the theoretical isotopic splitting of the complex $[Cu_2(\mathbf{2})(\mathbf{4})]^{2+}$.

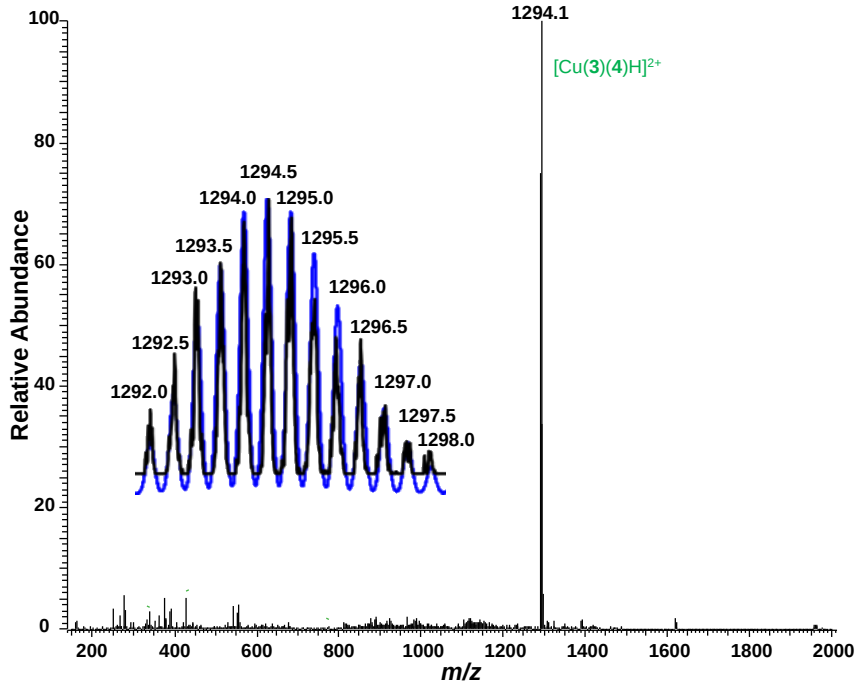

Figure S56. ESI-MS spectrum of compound **ROT-3** in CH_2Cl_2. The blue trace represents the theoretical isotopic splitting of the complex $[Cu(\mathbf{3})(\mathbf{4})H]^{2+}$.

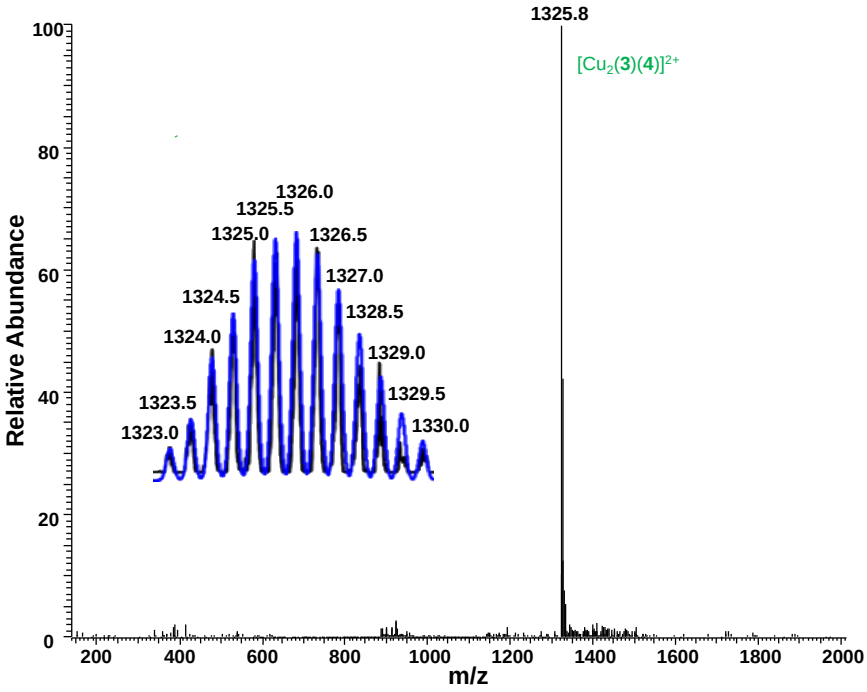

Figure S57. ESI-MS spectrum of compound **ROT-3'** in CH_2Cl_2. The blue trace represents the theoretical isotopic splitting of the complex $[Cu_2(\mathbf{3})(\mathbf{4})]^{2+}$.

6. Measurements of Binding Constants

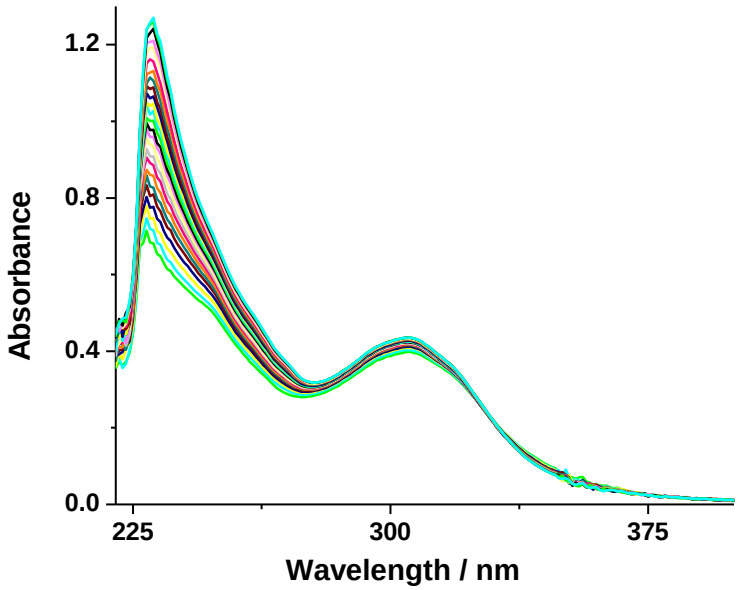

Figure S58. UV-Vis titration of **C1** (3×10^{-5} M) with **8** (10^{-3} M) in CH_2Cl_2 at 25 °C. log $K = 4.59 \pm 0.6$, $K = 3.89 \times 10^4$ M^{-1}.

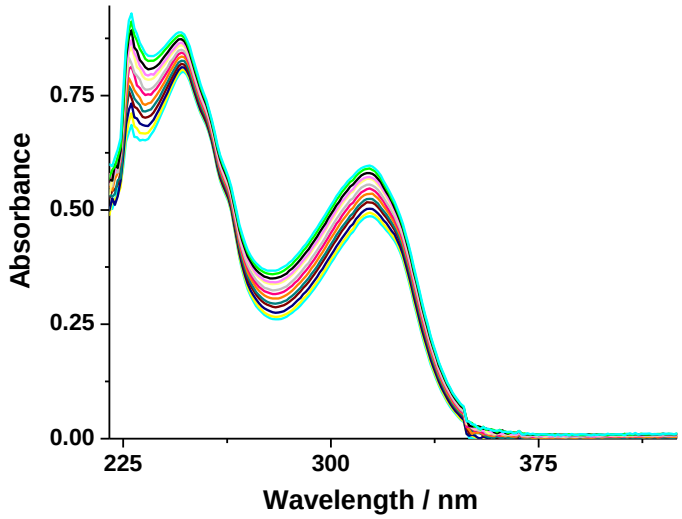

Figure S59. UV-Vis titration of **C1** (3×10^{-5} M) with **9** (10^{-3} M) in CH_2Cl_2 at 25 °C. log K = 2.93 ± 0.3, $K = 8.51 \times 10^2$ M^{-1}.

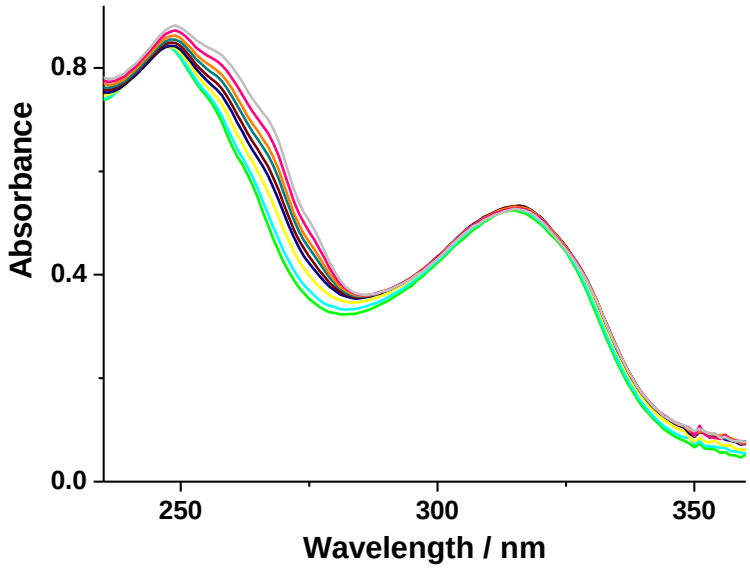

Figure S60. UV-Vis titration of **C1** (3×10^{-5} M) with **10** (10^{-3} M) in CH_2Cl_2 at 25 °C. log K = 4.10 ± 0.3, $K = 1.26 \times 10^4$ M^{-1}.

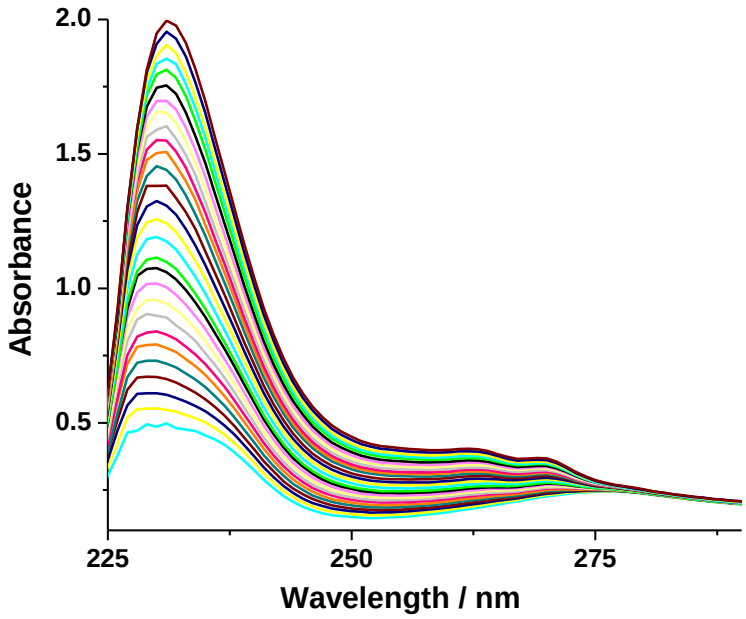

Figure S61. UV-Vis titration of **C5** (3×10^{-5} M) with **8** (10^{-3} M) in CH_2Cl_2 at 25 °C. log K = 4.63 ± 0.4, $K = 4.26 \times 10^4$ M^{-1}.

7. Hammett-type Correlation

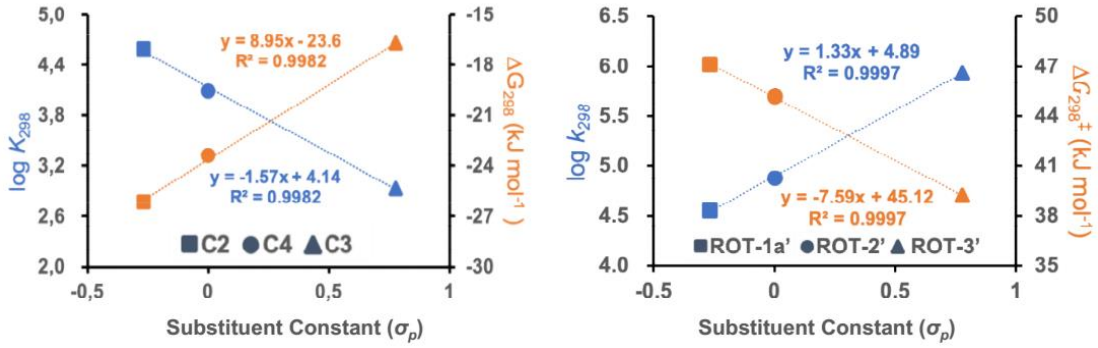

Figure S62. (Left) The binding constant and the Gibbs free energy correlate linearly with the substituent constant. (Right) The rotational frequency and the Gibbs free activation energy correlate linearly with the substituent constant.

8. References

1. Samanta, D.; Paul, I.; Schmittel, M. *Chem. Commun.* **2017**, *53*, 9709-9712.

2. Shi, Y.; Ke, Z.; Yeung, Y. Y. *Green. Chem.* **2018**, *20*, 295-297.

3. Youngblood, W. J.; Gryko, D. T.; Lammi, R. K.; Bocian, D. F.; Holten, D.; Lindsey, J. S. *J. Org. Chem.* **2002**, *67*, 2111-2117.

4. Ambroise, A.; Wanger, R. W.; Rao, P. D.; Riggs, J. A.; Hascoat, P.; Diers, J. R.; Seth, J.; Lammi, R. K.; Bocian, D. F.; Holten, D.; Lindsey, J. S. *Chem. Mater.* **2001**, *13*, 1023-1034.